Hadron production in pp collisions in the NICA energy range

V. Kolesnikov, V. Kireyeu, V. Lenivenko

K. Shtejer, E. Bratkovskaya

Outline

- ✓ Current state of the p+p experimental data at the NICA energy
- ✓ Model predictions of the excitation function of the hadron mean multiplicity from p+p collisions at the NICA energy range. Comparison with available data.

  Models: PHSD, Pythia 8.240, EPOS 1.99 and UrQMD 3.4

- ✓ Hadron p_T distributions from p+p collisions at $\sqrt{s}$ = 6.3, 7.6, 8.8, 12.3, 17.7 GeV, predicted by models and compared with NA61/SHINE data.

  Models: PHSD and Pythia 8.240

- ✓ Hadron rapidity distributions from p+p collisions at $\sqrt{s}$ = 6.3, 7.6, 8.8, 12.3, 17.7 GeV, predicted by models and compared with NA61/SHINE data.

  Models: PHSD and Pythia 8.240

- ✓ Parameterization of mean-multiplicity excitation functions of the available experimental data.
- ✓ Parameterization of rapidity distribution functions of the available experimental data.
- ✓ Parameterization of the slope parameter

$\sqrt{s} = 4 \div 27$ GeV

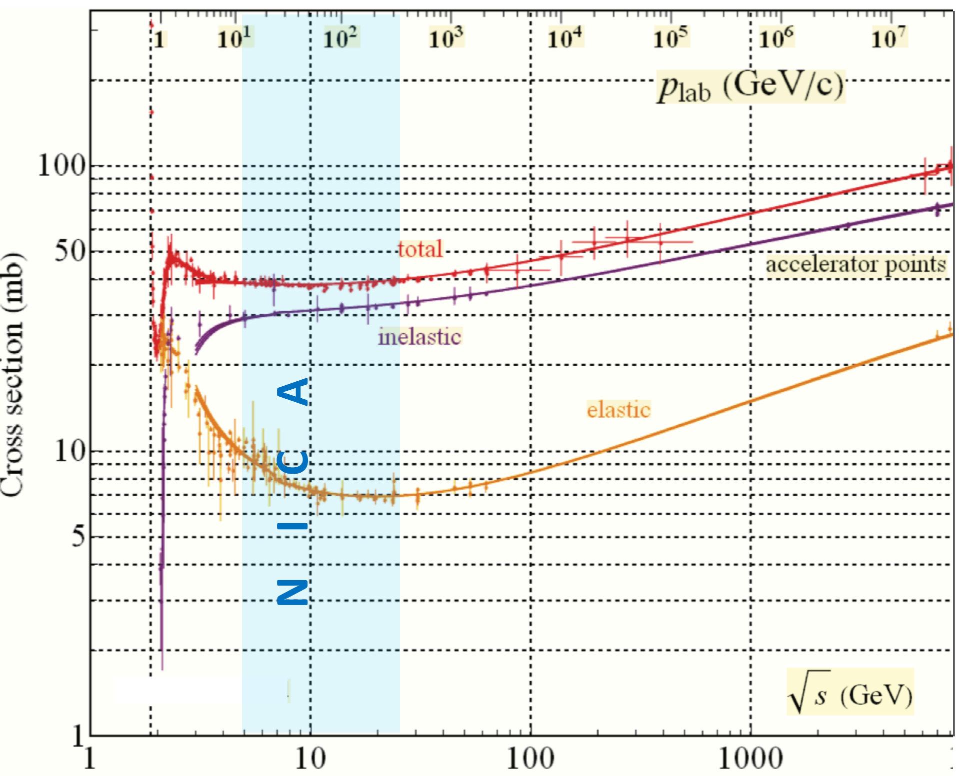

M. Tanabashi *et al.* (Particle Data) Phys. Rev. D **98**, 030001 (2018)

http://pdg.lbl.gov/2018/hadronic-xsections/rpp2018-pp_elastic.dat

http://pdg.lbl.gov/2018/hadronic-xsections/rpp2018-pp_total.dat

http://pdg.lbl.gov/2018/hadronic-xsections/

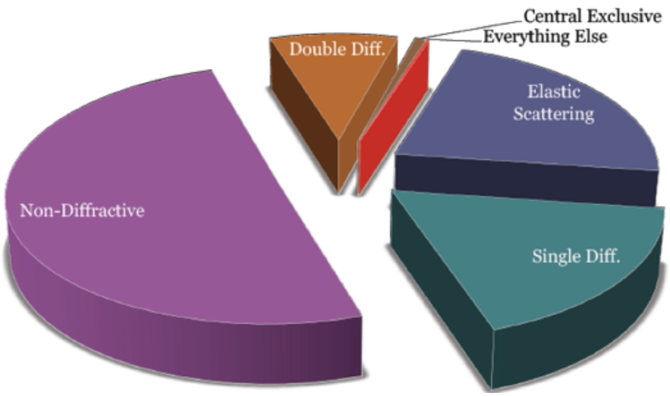

$$\sigma_{TOT} = \sigma_{el} + \overbrace{(\sigma_{SD} + \sigma_{DD} + \cdots) + \sigma_{ND}}^{\sigma_{inel}}$$

Inelastic cross section: p → ✳ ← p

Current state of the p+p experimental data at NICA energy range

Experiments aiming to measure multiparticle final states at $\sqrt{s}$ < 30 GeV have in common to contribute and learn about the non-perturbative QCD sector.

Even if the **inclusive** measurements account for the simplest contribution to the multidimensional phase-space, they are very important.

Data sets need to be precise and internally consistent, covering the whole available phase-space.

precision → Well defined error limits in the measured data, so that the resulting cross section data sets could be consistent within those limits.

↓

To allow to study the evolution of the inclusive yields from elementary to nuclear interactions.

↓

Most theoretical concepts for the interpretation of nuclear collisions rely on such experimental data as input for their calculations.

The comparison with elementary data is being significantly affected by the scarcity of p+p precise data in this energy region

Current state of the p+p experimental data at NICA energy range

Excitation function Hadron yields have been summarized in a range of $\sqrt{s_{pp}}$, from several GeV to LHC energies:

- A. M. Rossi et al., Nuclear Physics B84 (**1975**) 269 – 305.

"Experimental study of the energy dependence in proton-proton inclusive reactions"

Energy dependence of charge particle production in p+p inclusive reactions:

$$\left.\begin{array}{l} p+p\to\pi^{\pm}+X \\ p+p\to K^{\pm}+X \\ p+p\to p^{\pm}+X \end{array}\right\} \sqrt{s} = 3 \div 53 \text{ GeV}$$

Data from CERN ISR (single arm spectrometer) and bubble chambers (1962 - 1971)

- M. Gazdzicki and D. Roehrich, Z. Phys. C71 (**1996**) 55 – 64.

"Strangeness in Nuclear Collisions"

Mean multiplicity of strange hadrons produced in p+p collisions:

$$p+p\to\begin{bmatrix} K^{\pm} \\ \Lambda \\ \overline{\Lambda} \\ K_s^0 \end{bmatrix} \sqrt{s} = 2 \div 28 \text{ GeV}$$

Data from CERN ISR , bubble and streamer chambers

- H. Weber et al., Phys. Rev. C 67 (**2003**) 014904.

"Hadronic observables from SIS to SPS energies – anything strange with strangeness?"

Mean multiplicity of strange hadrons produced in p+p collisions

Current state of the p+p experimental data at NICA energy range

Experiments that have measured inclusive particle yield from proton-proton interactions:

FermiLab (FNAL)

Bubble chambers

- the statistics is restricted to small data samples of about 10^4 events (30 inch bubble chamber).
- the particle identification is mostly absent.

Spectrometers

- small solid angle devices.
- well defined ranges of production angles.
- complete particle identification by means of Cerenkov and Scintillator counters along with proportional chambers inside the spectrometer.

→ measured inelastic pp events at 100 ÷ 400 GeV/c corresponding to $\sqrt{s}$ = 14 ÷ 27 GeV

CERN Intersecting Storage Rings (ISR) 1971 - 1984 → measured elastic and inelastic pp and $p\bar{p}$ events at $\sqrt{s}$ = 23.6 ÷ 62.2 GeV.

CERN SPS NA49 → inelastic pp interactions at p_{beam} = 158 GeV/c (equivalent to $\sqrt{s} = 17.3$ GeV)

CERN SPS NA61/SHINE → inelastic pp interactions:

p_{beam} (GeV/c)	20	31	40	80	158
$\sqrt{s}$ (GeV)	6.27	7.74	8.76	12.32	17.27

The largest collection of experimental proton-proton cross sections at energies below 30 GeV was obtained with

- bubble chambers
- spectrometers
- CERN ISR collider.

However, detailed information about particle production from proton-proton at $\sqrt{s}$ =10 ÷ 30 GeV might be not sufficient:

- ✓ sparse
- ✓ mainly refer to basic features of unidentified charged hadron production
- ✓ the results on identified hadron spectra, fluctuations and correlations are mostly missing
- ✓ the tracking is not precise: experiments between 1970 and 1980 measured cross sections without any correction for feed-down products from strange weak decays.

Motivation:

- ✓ Interpretation of experimental results from nucleus-nucleus interactions showing novel phenomena has to rely on the comparison to the corresponding data from elementary collisions.
- ✓ Microscopic models of nucleus-nucleus collisions are useful tools for explaining experimental results and making new predictions. Data on hadron yields from elementary inelastic collisions ate the essential input for such kind of models.
- ✓ There are several review papers, which summarize data from p+p and discuss the excitation function of hadron yields in a range of collision energies from several GeV up to LHC energies.

But …

- ✓ They rely on a too broad region of energies as compared to the NICA range and do not include the recent measurements from CERN/SPS.
- ✓ The data from NA61 and NA49 (> 6 papers) allow detailed examination of total yield, rapidity and p_T spectra:

[9] C. Alt et al (NA49 Collaboration) Eur. Phys.J. C45 (2006) 343-381.

[10] T. Anticic et al (NA49 Collaboration) Eur. Phys. J. C (2010) 68: 1-73.

[11] T. Anticic et al (NA49 Collaboration) Eur. Phys. J. C (2010) 65: 9-63.

[13] N. Abgrall et al (NA61/SHINE Collaboration), Eur. Phys. J. C (2014) 74:2794.

[14] A. Aduszkiewicz et al (NA61/SHINE Collaboration), Eur. Phys. J. C (2017) 77:671.

[15] A. Aduszkiewicz et al (NA61/SHINE Collaboration), Eur. Phys. J. C (2016) 76:198

- ✓ New look to the $\pi^-$from h-minus (more data on pions)

The aim of this study is twofold.

- First, in order to improve the existing elementary data base we want to collect the most complete set of experimental data of hadron yields from p+p collisions in the NICA energy range, which includes results of mean multiplicities, rapidity distributions, and transverse spectra.

- Secondly, we want to undertake a systematic study of the collected experimental results as a function of the collision energy and obtain proper parameterizations for the energy dependence of inclusive production cross-sections, as well as investigate the evolution of the parameters of the hadron phase-space distributions (i.e. shapes of rapidity spectra and transverse momentum distributions).

- Since most bulk observables relate to the non-perturbative sector of QCD, it is one of the main goals of this work to obtain the basis for a model independent framework for predicting of hadron yields in p+p collisions at NICA energies.

- Thus, the results of this study can be used as an input for detector simulation and feasibility study at NICA.

Reference	$\sqrt{s_{NN}}$ (GeV)	$\langle\pi^-\rangle$	Error (%)
[6, 19]	2.99	0.2	10
[6, 19]	3.50	0.29	10
[6, 19]	4.93	0.63	10
[6, 19]	5.03	0.75	10
[19]	5.10	0.72	10
[19]	5.97	0.98	10
[6, 19]	6.12	1.01	10
[13]	6.27	1.05	5
[14]	6.27	1.08	19
[19]	6.38	1.08	10
[6, 19]	6.84	1.11	10
[19]	6.86	1.11	10
[19]	7.43	1.21	10
[13]	7.74	1.31	5
[14]	7.75	1.47	13
[13]	8.76	1.48	3
[14]	8.76	1.71	10
[13]	12.32	1.94	4
[14]	12.32	2.03	9
[6, 19]	13.90	2.19	10
[13]	17.30	2.44	5
[14]	17.30	2.40	8
[10]	17.30	2.36	2
[19]	19.75	2.82	10
[19]	22.02	2.98	10
[10, 19]	30.98	3.44	10

Reference	$\sqrt{s_{NN}}$ (GeV)	$\langle\pi^+\rangle$	Error (%)
[6, 19]	2.99	0.48	10
[6, 19]	3.50	0.67	10
[6, 19]	4.93	1.22	10
[6, 19]	5.03	1.37	10
[6, 19]	6.12	1.6	10
[14]	6.27	1.88	11
[6, 19]	6.84	1.88	10
[14]	7.75	2.08	10
[14]	8.76	2.39	7
[14]	12.32	2.67	5
[14]	17.30	3.11	13
[10]	17.30	3.02	2
[19]	22.02	3.56	10
[10, 19]	30.98	4.04	10

Table 1: The compiled results on the mean multiplicity of charged pions from inelastic proton-proton interactions at different collision energies.

Reference	$\sqrt{s_{NN}}$ (GeV)	$\langle K^-\rangle$	Error (%)
[6, 19]	5.03	0.0095	35
[6, 19]	6.15	0.036	14
[14]	6.27	0.024	26
[6, 19]	6.84	0.031	14
[14]	7.75	0.045	11
[6]	7.86	0.05	30
[6, 19]	8.21	0.07	29
[14]	8.76	0.084	8
[6, 19]	9.08	0.08	25
[6, 19]	9.97	0.11	27
[6, 19]	11.54	0.13	23
[14]	12.32	0.095	7
[14]	17.30	0.132	11
[10]	17.30	0.13	10
[19]	22.02	0.24	10
[10]	23.00	0.171	15
[6]	23.68	0.209	15
[6]	30.59	0.244	15
[10, 19]	30.98	0.245	10

Reference	$\sqrt{s_{NN}}$ (GeV)	$\langle K^+\rangle$	Error (%)
[6]	2.98	0.0046	15
[6, 19]	2.99	0.0035	16
[6]	2.99	0.0044	18
[6]	3.12	0.0057	18
[6]	3.35	0.0069	15
[6, 19]	3.50	0.008	21
[6]	4.11	0.02	20
[6, 19]	5.03	0.07	43
[6]	5.35	0.054	10
[6, 19]	6.15	0.107	2
[14]	6.27	0.097	14
[6, 19]	6.84	0.1188	1 3
[14]	7.75	0.157	12
[14]	8.76	0.17	15
[6, 19]	11.54	0.21	28
[14]	12.32	0.201	7
[14]	17.30	0.234	9
[10]	17.30	0.227	5
[19]	22.02	0.35	10
[10]	23.00	0.273	15
[6]	23.68	0.337	15
[6]	30.59	0.367	15
[10, 19]	30.98	0.3562	13

Table 2: The compiled results on the mean multiplicity of charged kaons from inelastic proton-proton interactions at different collision energies.

Reference	$\sqrt{s_{NN}}$ (GeV)	$\langle K^0_S\rangle$	Error (%)
[6]	2.98	0.00083	22
[6]	3.35	0.0019	16
[6, 19]	3.50	0.00364	3
[6]	3.63	0.0034	9
[6]	3.85	0.0064	8
[6]	4.08	0.0072	8
[6, 19]	4.93	0.0202	2
[6, 19]	5.01	0.023	2
[6, 19]	6.12	0.0415	3
[6, 19]	6.84	0.0495	2
[6]	6.91	0.045	9
[6]	11.45	0.109	6
[6]	13.76	0.122	8
[6, 19]	13.90	0.141	10
[6]	16.66	0.158	4
[6]	19.42	0.16	13
[6]	19.66	0.181	8
[10]	23.00	0.222	10
[6]	23.76	0.224	8
[6]	26.02	0.26	4
[6]	27.43	0.2	10
[6]	27.60	0.232	5
[10, 19]	30.98	0.274	10

Reference	$\sqrt{s_{NN}}$ (GeV)	$\langle\Lambda\rangle$	Error (%)
[6]	2.98	0.0033	18
[25]	3.17	0.0073	4
[6]	3.35	0.0073	4
[6, 19]	3.50	0.0127	9
[6]	3.63	0.0109	6
[6]	3.85	0.0172	6
[6]	4.08	0.0201	5
[6, 19]	4.93	0.0388	2
[6, 19]	5.01	0.035	11
[6, 19]	6.12	0.061	3
[6, 19]	6.84	0.0657	1
[6]	6.91	0.037	19
[6]	11.45	0.109	6
[6]	13.76	0.112	12
[6, 19]	13.90	0.099	12
[6]	16.66	0.133	5
[14]	17.30	0.12	9
[6]	19.42	0.08	25
[6]	19.66	0.103	11
[6]	23.76	0.111	14
[6]	23.76	0.11	9
[6]	26.02	0.12	17
[6]	27.43	0.12	8
[6]	27.60	0.125	6

Table 3: The compiled results on the mean multiplicity of $\langle K^0_S\rangle$ and $\langle\Lambda\rangle$ from inelastic proton-proton interactions at different collision energies.

Reference	$\sqrt{s_{NN}}$ (GeV)	$\langle p\rangle$	Error (%)
[6, 19]	3.50	1.56	10
[6, 19]	4.93	1.68	10
[6, 19]	5.01	1.55	10
[6, 19]	6.12	1.41	10
[6, 19]	6.15	1.69	10
[14]	6.27	1.154	4
[6, 19]	6.84	1.615	10
[14]	7.75	1.093	6
[14]	8.76	1.095	8
[14]	12.32	0.977	14
[14]	17.30	1.069	12
[10]	17.30	1.162	15
[19]	22.02	1.28	10
[10, 19]	30.98	1.34	10

Reference	$\sqrt{s_{NN}}$ (GeV)	$\langle\bar{p}\rangle$	Error (%)
[6, 19]	6.15	0.0023	10
[14]	6.27	0.0047	15
[6, 19]	6.84	0.004	10
[14]	7.75	0.0047	16
[6, 19]	8.21	0.005	10
[14]	8.76	0.0059	12
[6, 19]	9.08	0.008	10
[6, 19]	9.97	0.011	10
[6, 19]	11.54	0.015	10
[14]	12.32	0.0183	10
[14]	17.30	0.0402	9
[10]	17.30	0.039	15
[19]	22.02	0.061	10
[10, 19]	30.98	0.11	10

Table 4: The compiled results on the mean multiplicity of $\langle p\rangle$ and $\langle\bar{p}\rangle$ from inelastic proton-proton interactions at different collision energies.

Mean multiplicity *vs* collision energy

Predictions from **PHSD**, **Pythia 8.240**, **EPOS 1.99** and **UrQMD 3.4** are compared with experimental data.

$K^{\pm}, \pi^{\pm}$

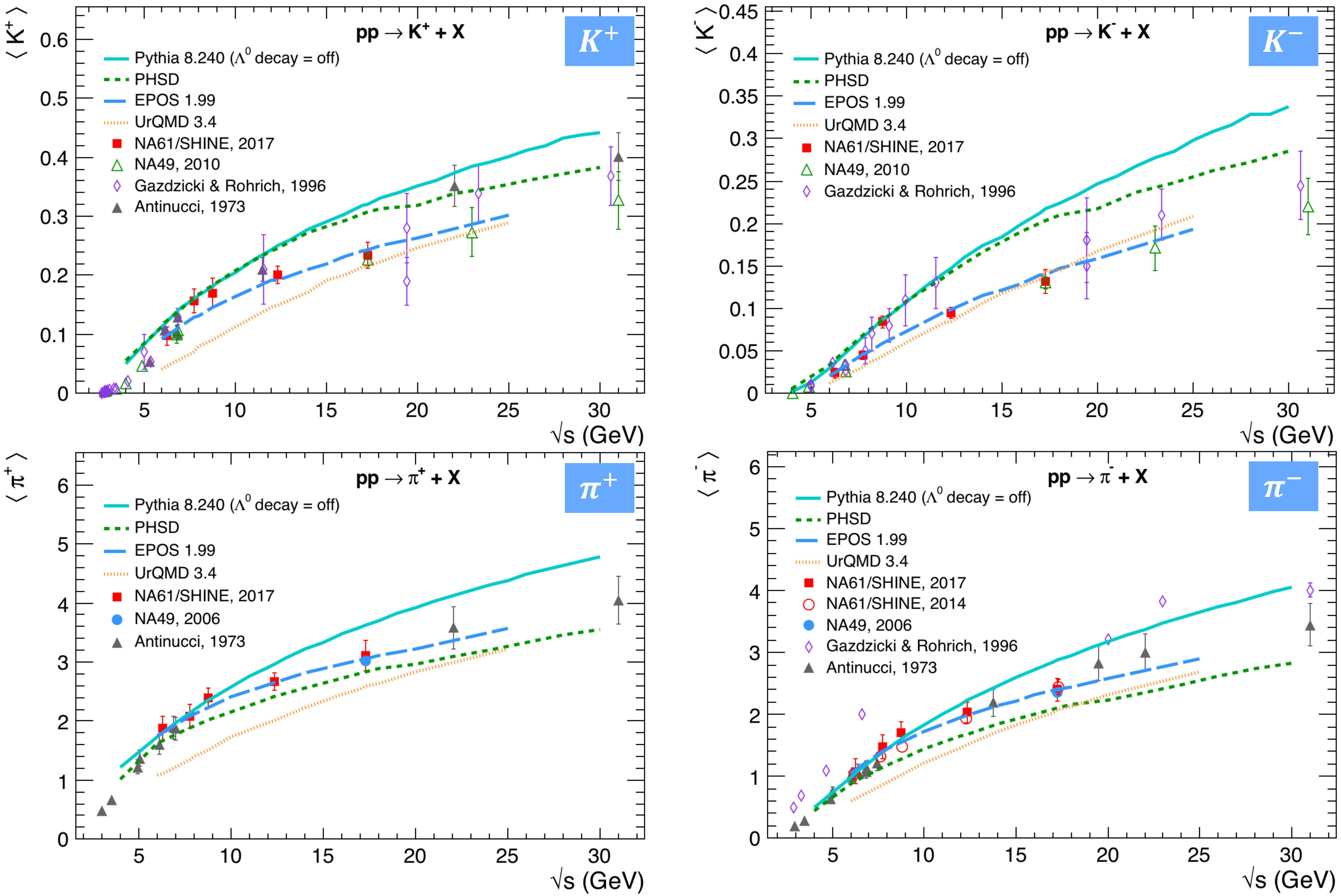

Mean multiplicity *vs* collision energy

Predictions from **PHSD**, Pythia 8.240, **EPOS 1.99** and **UrQMD 3.4** are compared with experimental data.

$\boldsymbol{p}, \overline{\boldsymbol{p}}$

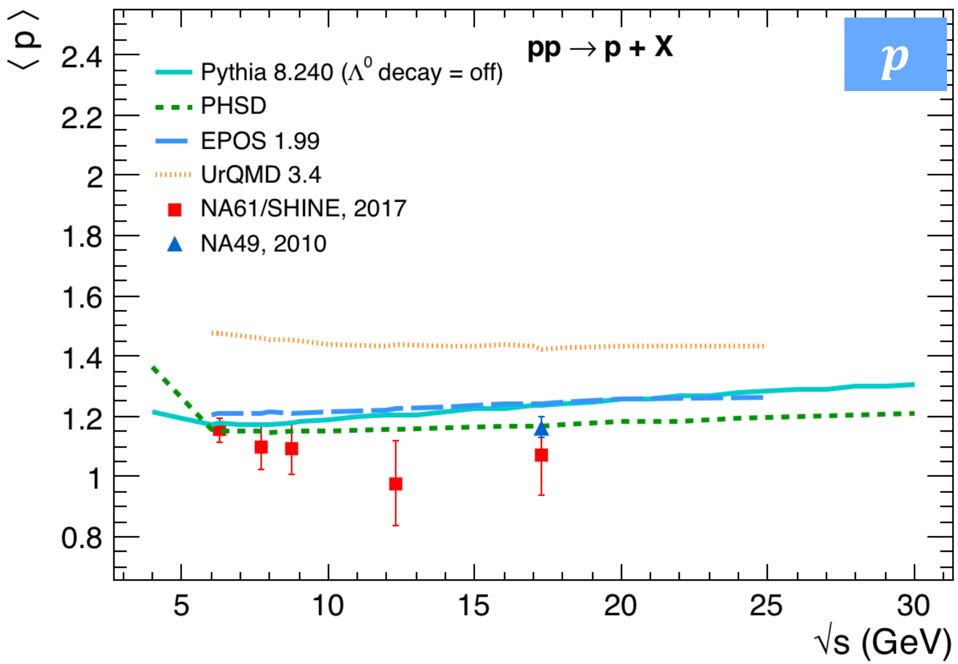

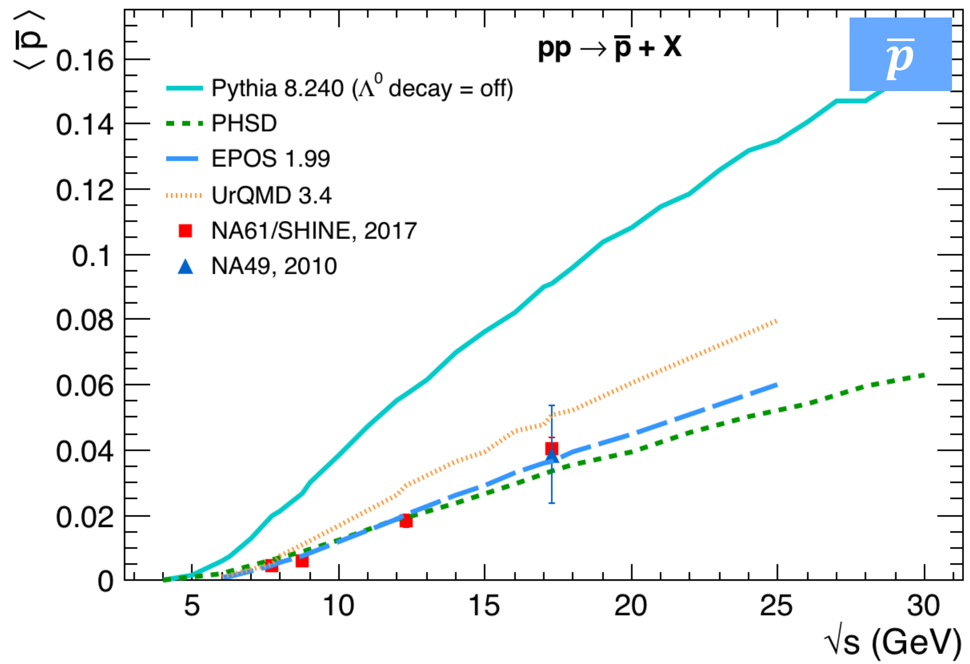

PHSD is more consistent with the experimental results of proton production from pp collisions.

PHSD and EPOS are more in agreement with the data, while Pythia overestimates the $\overline{p}$ yield in a large extent.

Mean multiplicity *vs* collision energy

Contribution of π^+ and π^- from K_0^s weak decay, predicted by Pythia 8.240 and **PHSD**.

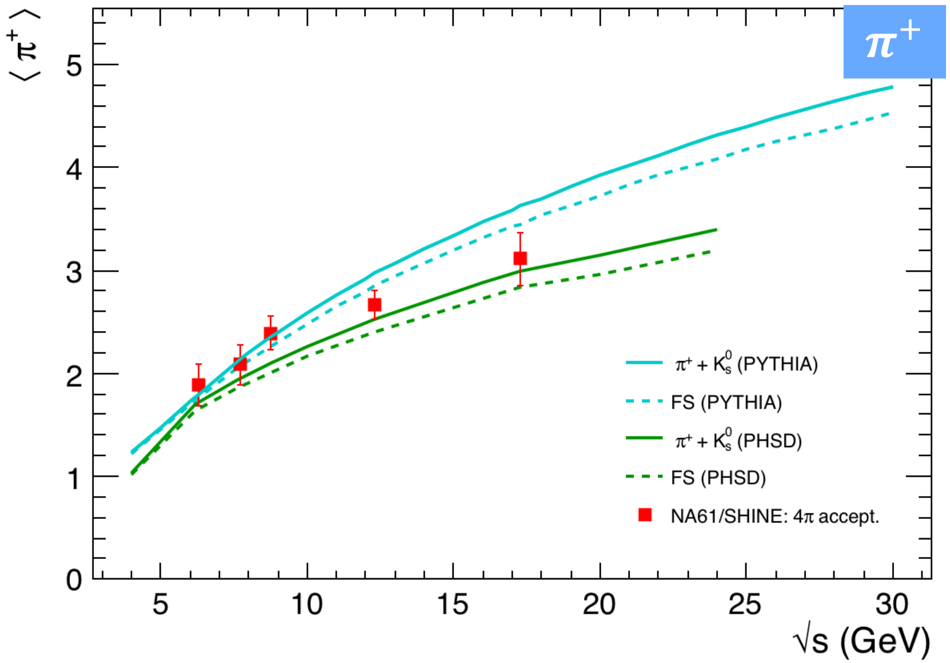

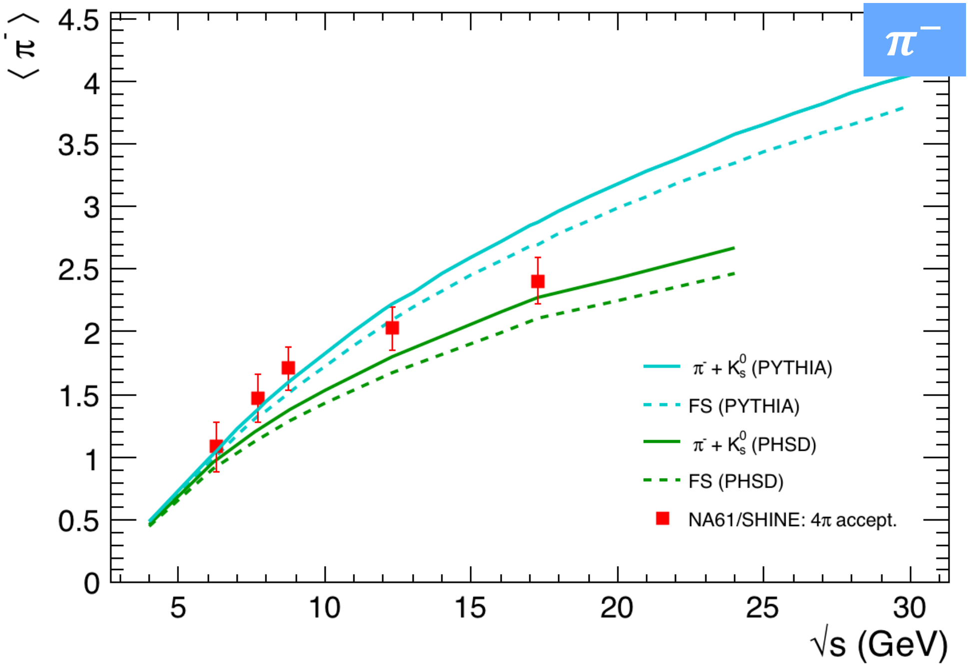

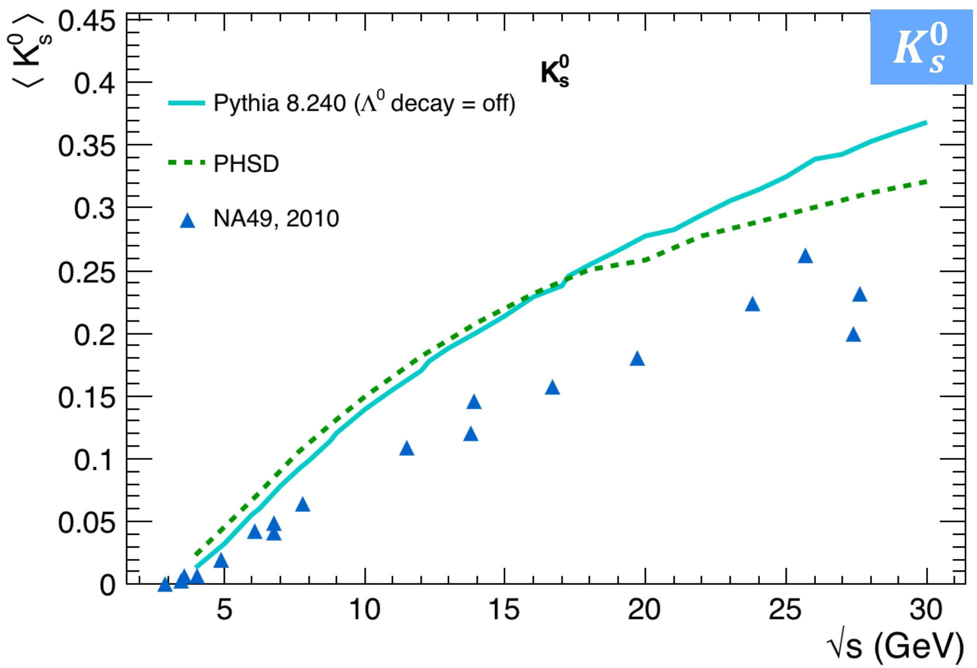

The $\pi^\pm$ yield obtained with Pythia, includes the contribution of the final state (FS) pions as well as the contribution from K_0^S which primarily decays into two pions.

Predictions from **PHSD**, **Pythia 8.240** and **EPOS 1.99** are compared with experimental data.

The result from NA61/SHINE was corrected for particles from weak decays (feed-down).

$$\Xi^- \rightarrow \Lambda^0 + \pi^- \ (99.8\%)$$

$$\Xi^0 \rightarrow \Lambda^0 + \pi^0 \ (99.5\%)$$

The feed-down correction in NA61/SHINE was based on the **EPOS model** which described well the available cross section data for strange particles.

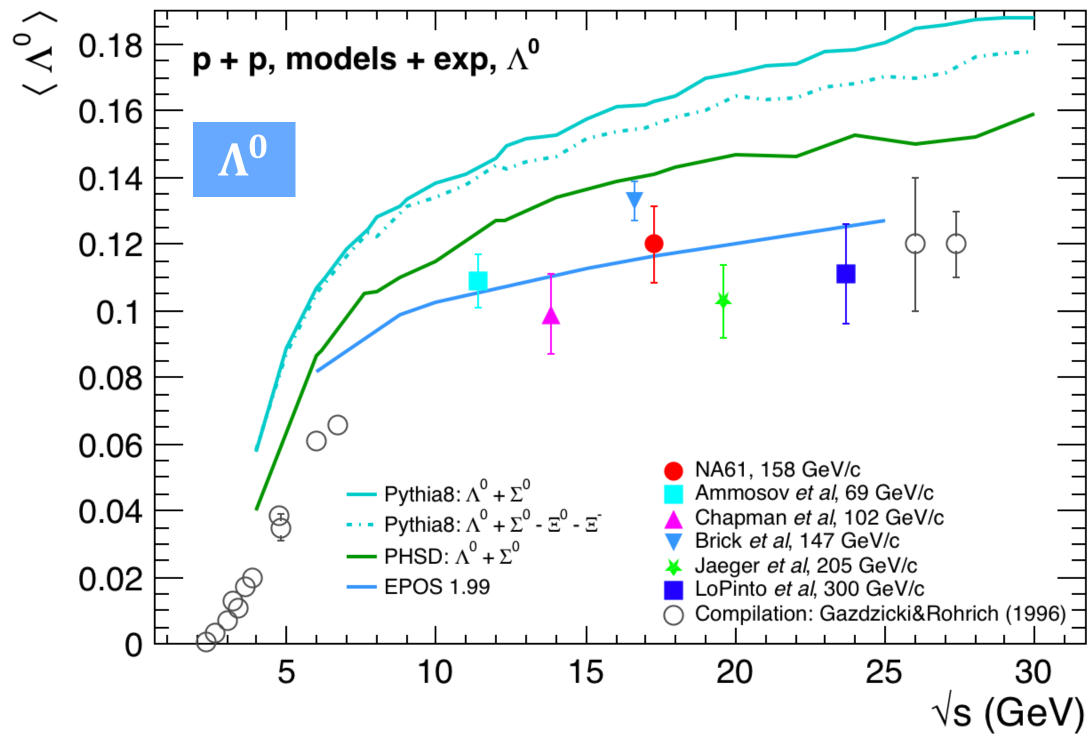

Feed-down corrections for other hadron multiplicities should be done with models, but the lack of precise knowledge of the production cross section of the following particles, contributes to systematic errors in the measurements:

$$\boldsymbol{K}^+ \rightarrow \boldsymbol{\pi}^+ + \pi^0 \ (20.6\%)$$

$$\boldsymbol{K}^- \rightarrow \boldsymbol{\pi}^- + \pi^0 \ (20.6\%)$$

$$K_S^0 \rightarrow \boldsymbol{\pi}^+ + \boldsymbol{\pi}^- \ (69.2\%)$$

$$\Lambda^0 \rightarrow \boldsymbol{p} + \boldsymbol{\pi}^- \ (64\%)$$

$$\overline{\Lambda^0} \rightarrow \overline{\boldsymbol{p}} + \boldsymbol{\pi}^+$$

$$\Sigma^- \rightarrow n + \boldsymbol{\pi}^- \ (100\%)$$

$$\Sigma^+ \begin{cases} \boldsymbol{p} + \pi^0 \ (52\%) \\ n + \boldsymbol{\pi}^+ \ (48\%) \end{cases}$$

Transverse momentum, p_T spectra

π^- from Inelastic p + p collisions at $\sqrt{s}$ = 6.3, 7.6, 8.8, 12.3, 17.7 GeV

Experimental data from **NA61/SHINE** ($0 < y < 0.2$)

Predictions from **PHSD** and **PYTHIA**

PHSD contributions from different channels: decays from B-B strings and resonance decays

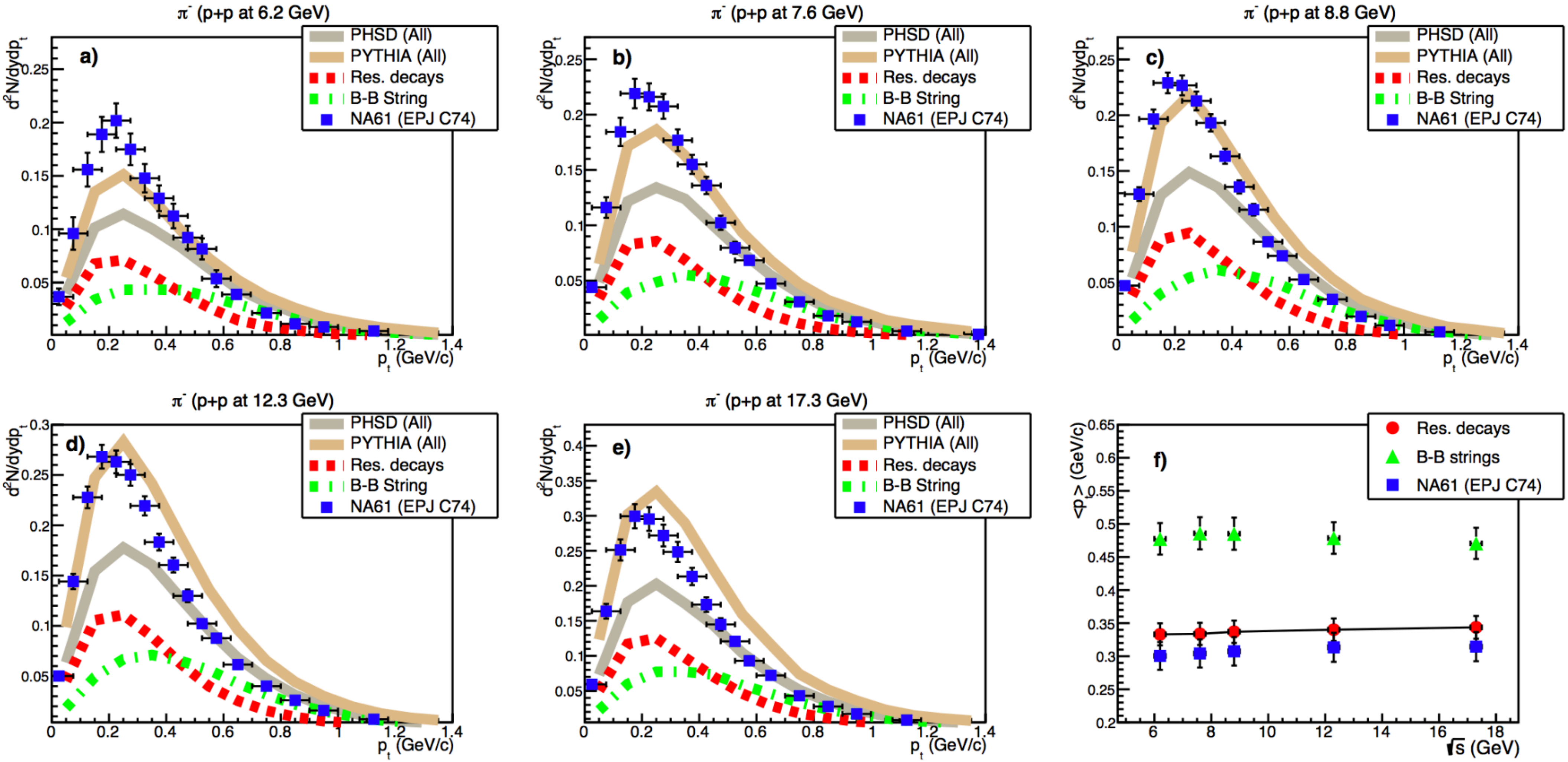

Hadrons from B-B strings have larger $\langle p_T \rangle$

Hadrons from resonance decays exhibit a p_T spectra similar to the data.

Transverse momentum, p_T spectra

K^- from Inelastic p + p collisions at $\sqrt{s}$ = 6.3, 7.6, 8.8, 12.3, 17.7 GeV

Experimental data from **NA61/SHINE** ($0 < y < 0.2$)

Predictions from **PHSD** and **PYTHIA**

PHSD contributions from different channels: decays from B-B strings and resonance decays

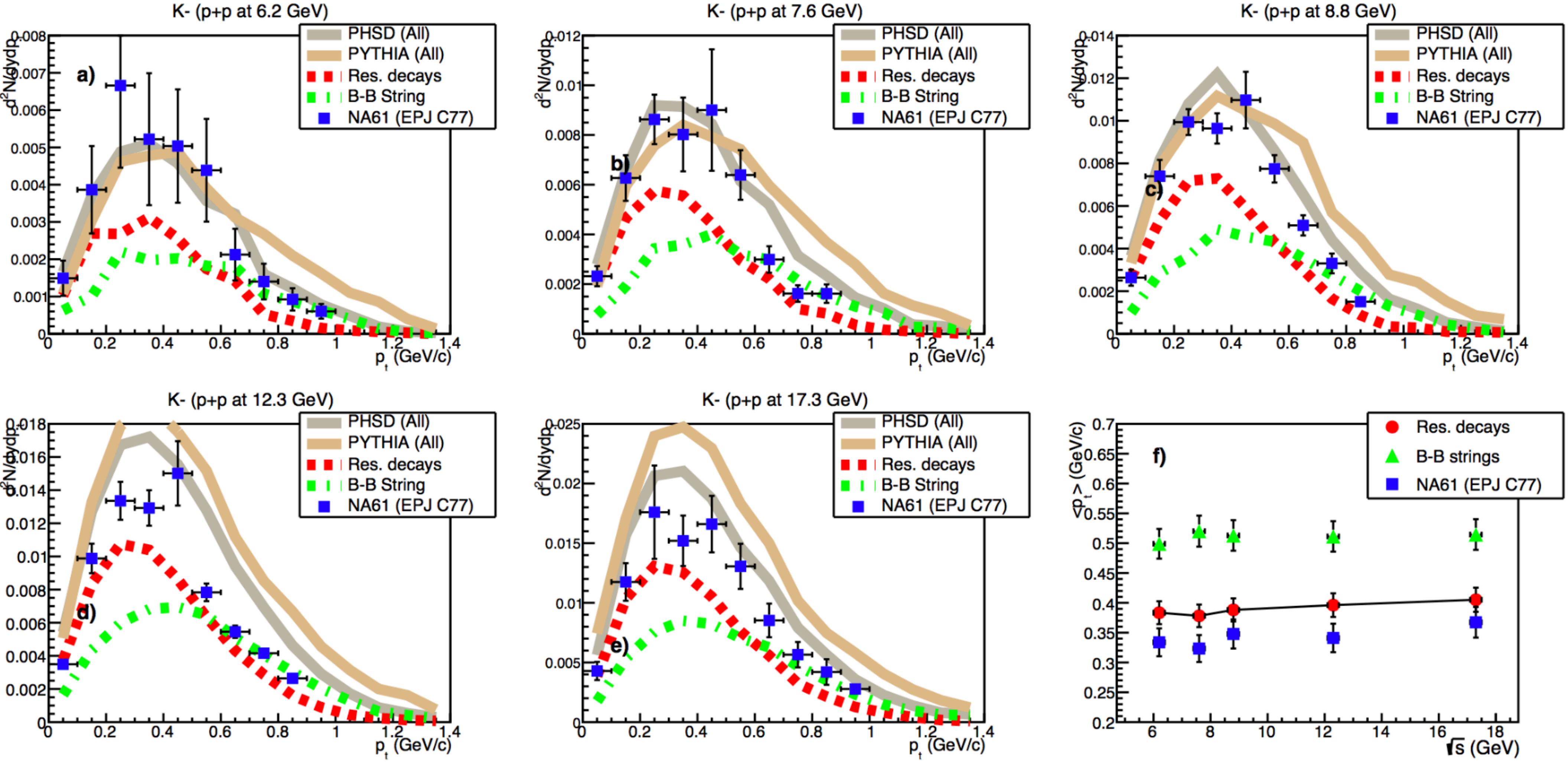

Hadrons from B-B strings have larger $\langle p_T \rangle$

Hadrons from resonance decays exhibit a p_T spectra similar to the data.

Transverse momentum, p_T spectra

K^+ from Inelastic p + p collisions at $\sqrt{s}$ = 6.3, 7.6, 8.8, 12.3, 17.7 GeV

Experimental data from **NA61/SHINE** ($0 < y < 0.2$)

Predictions from **PHSD** and **PYTHIA**

PHSD contributions from different channels: decays from B-B strings and resonance decays

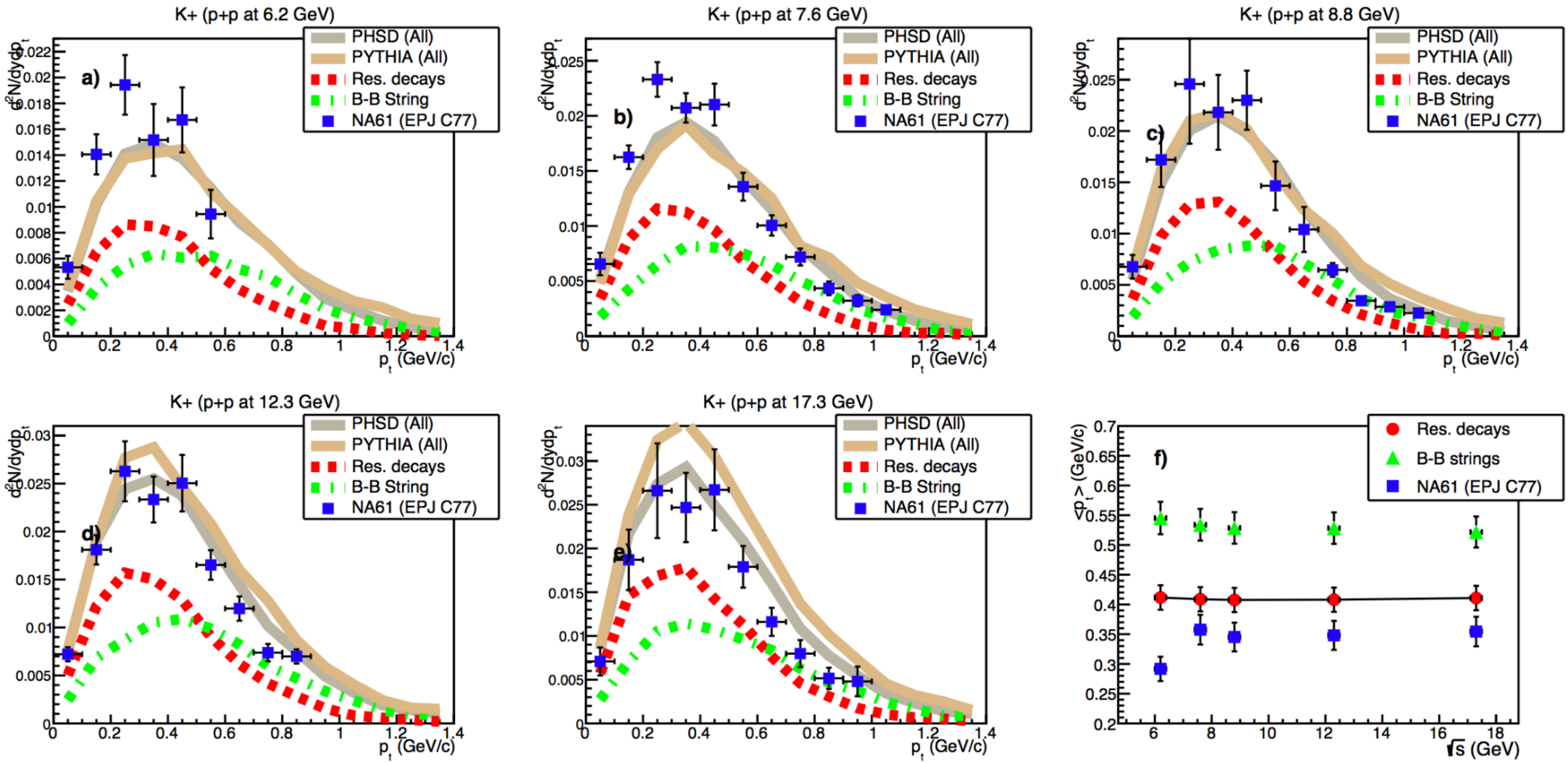

Hadrons from B-B strings have larger $\langle p_T \rangle$

Hadrons from resonance decays exhibit a p_T spectra similar to the data.

Transverse momentum, p_T spectra

Protons from Inelastic p + p collisions at $\sqrt{s}$ = 6.3, 7.6, 8.8, 12.3, 17.7 GeV

Experimental data from **NA61/SHINE** ($0 < y < 0.2$)

Predictions from **PHSD** and **PYTHIA**

PHSD contributions from different channels: decays from B-B strings and resonance decays

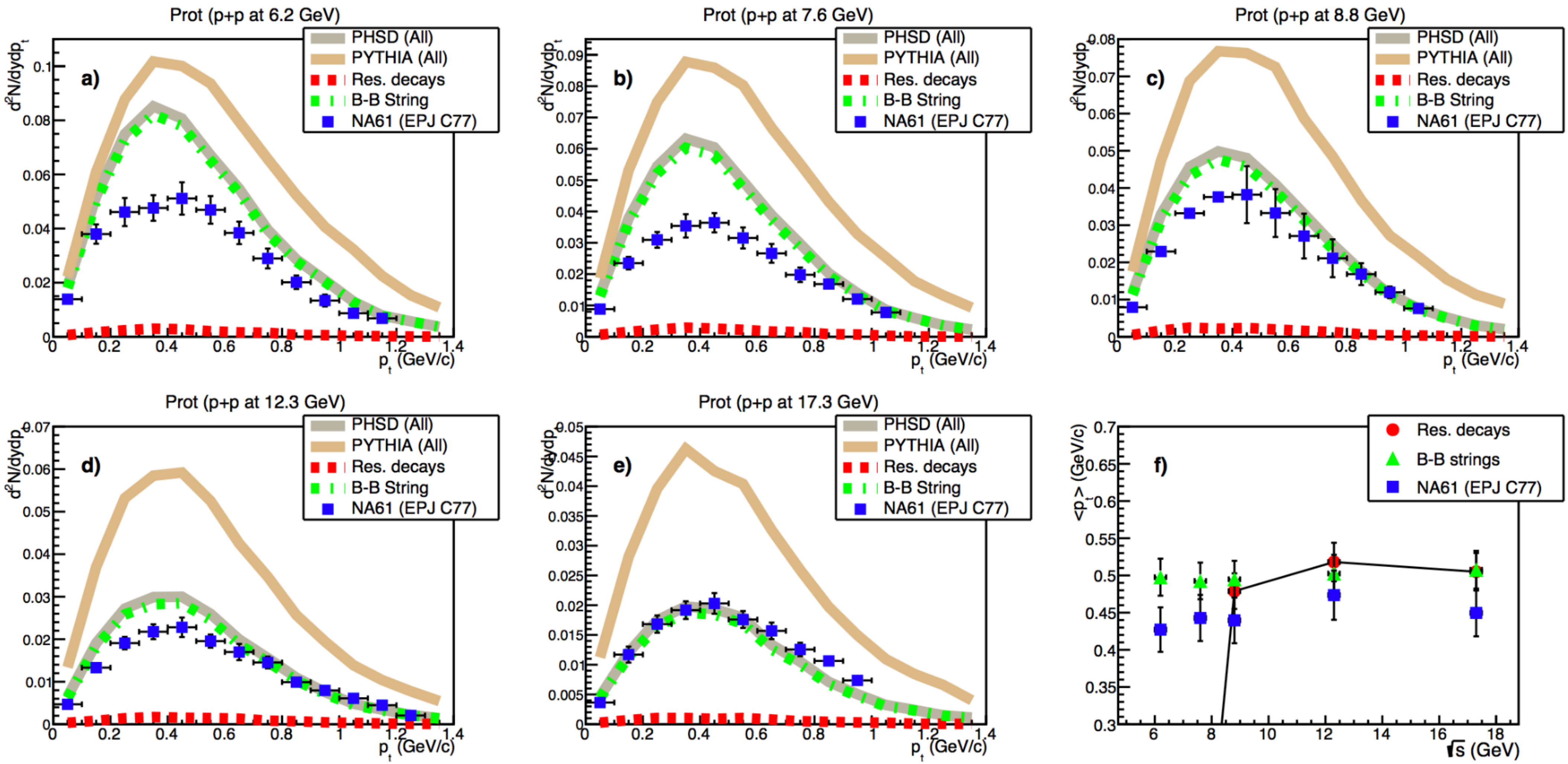

Hadrons from B-B strings have larger $\langle p_T \rangle$

Hadrons from resonance decays exhibit a p_T spectra similar to the data.

π^-

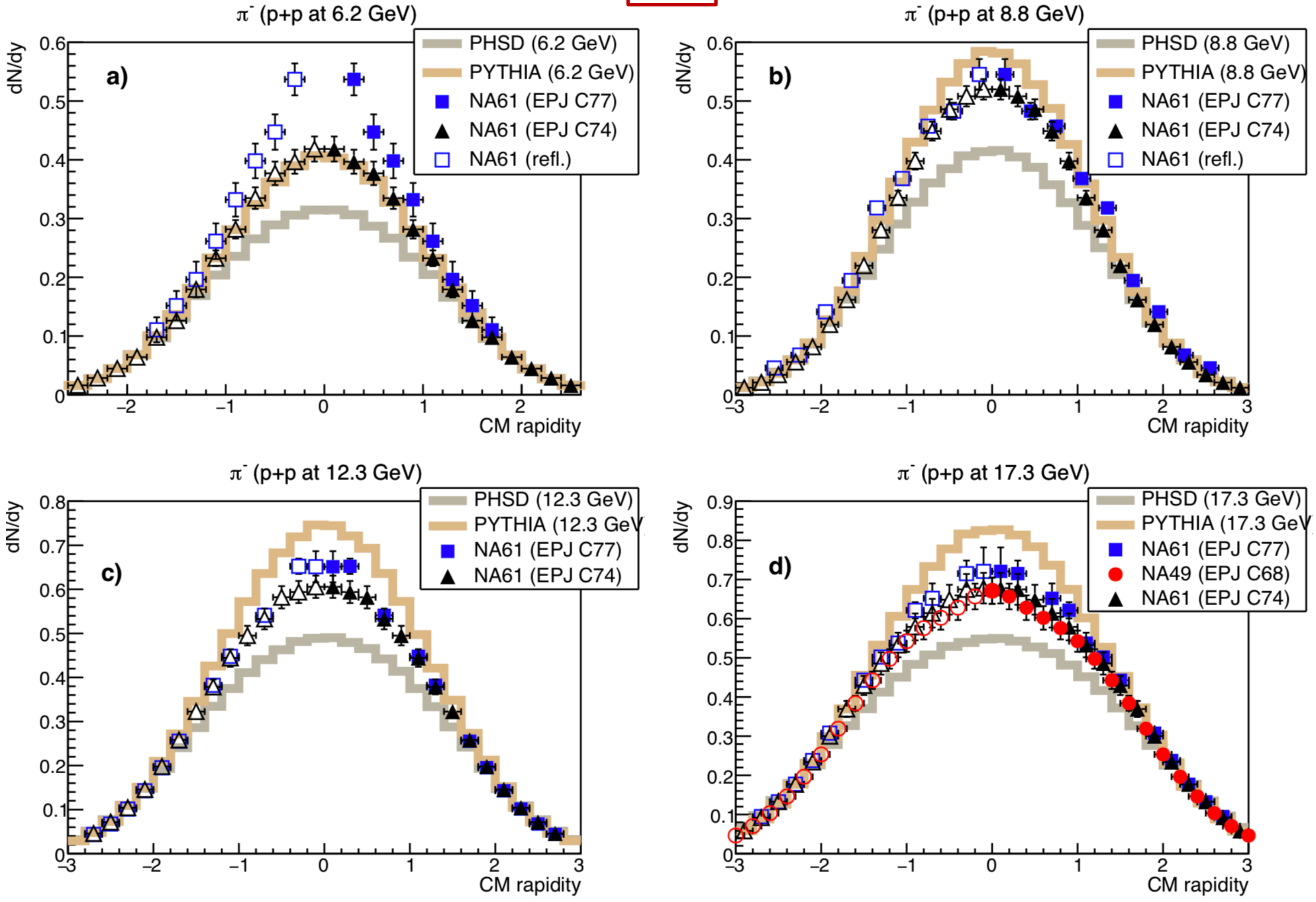
π⁻ (p+p at 6.2 GeV)
a)
PHSD (6.2 GeV)
PYTHIA (6.2 GeV)
NA61 (EPJ C77)
NA61 (EPJ C74)
NA61 (refl.)
dN/dy
CM rapidity
π⁻ (p+p at 8.8 GeV)
b)
PHSD (8.8 GeV)
PYTHIA (8.8 GeV)
NA61 (EPJ C77)
NA61 (EPJ C74)
NA61 (refl.)
dN/dy
CM rapidity
π⁻ (p+p at 12.3 GeV)
c)
PHSD (12.3 GeV)
PYTHIA (12.3 GeV)
NA61 (EPJ C77)
NA61 (EPJ C74)
dN/dy
CM rapidity
π⁻ (p+p at 17.3 GeV)
d)
PHSD (17.3 GeV)
PYTHIA (17.3 GeV)
NA61 (EPJ C77)
NA49 (EPJ C68)
NA61 (EPJ C74)
dN/dy
CM rapidity

π^+

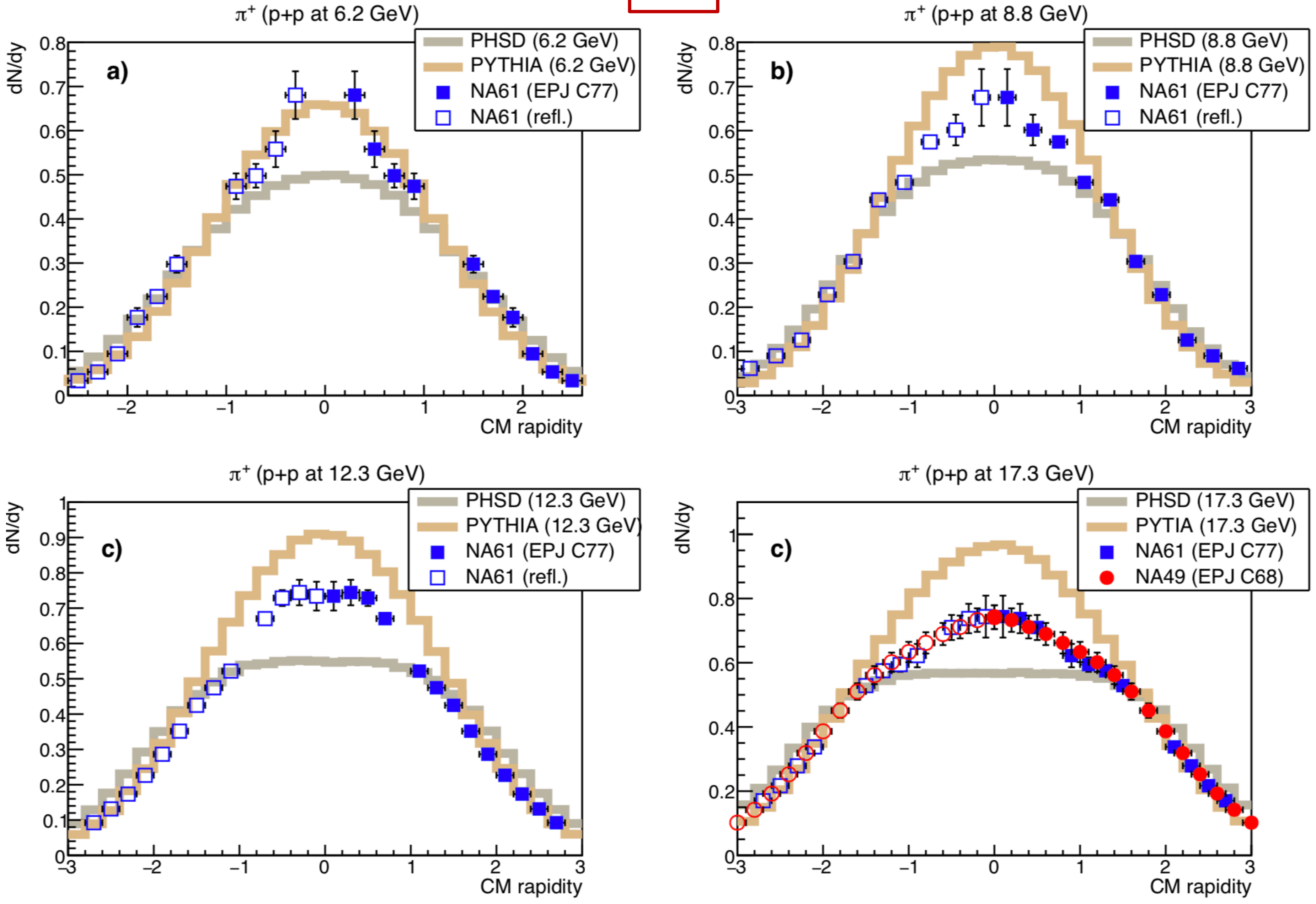
π+ (p+p at 6.2 GeV)
PHSD (6.2 GeV)
PYTHIA (6.2 GeV)
NA61 (EPJ C77)
NA61 (refl.)
a)
dN/dy
CM rapidity
π+ (p+p at 8.8 GeV)
PHSD (8.8 GeV)
PYTHIA (8.8 GeV)
NA61 (EPJ C77)
NA61 (refl.)
b)
dN/dy
CM rapidity
π+ (p+p at 12.3 GeV)
PHSD (12.3 GeV)
PYTHIA (12.3 GeV)
NA61 (EPJ C77)
NA61 (refl.)
c)
dN/dy
CM rapidity
π+ (p+p at 17.3 GeV)
PHSD (17.3 GeV)
PYTIA (17.3 GeV)
NA61 (EPJ C77)
NA49 (EPJ C68)
c)
dN/dy
CM rapidity

Rapidity distributions

K^-

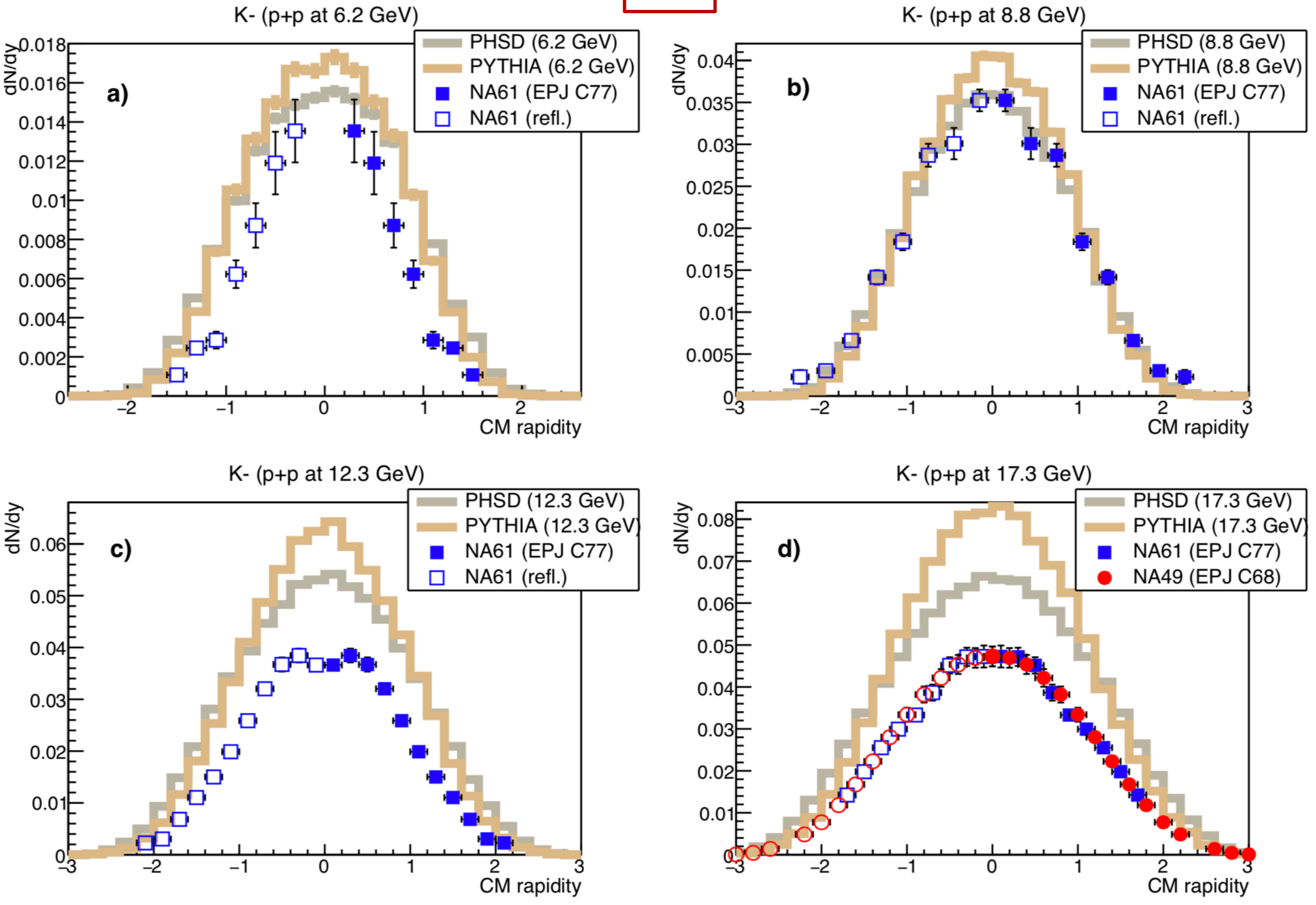

K^+

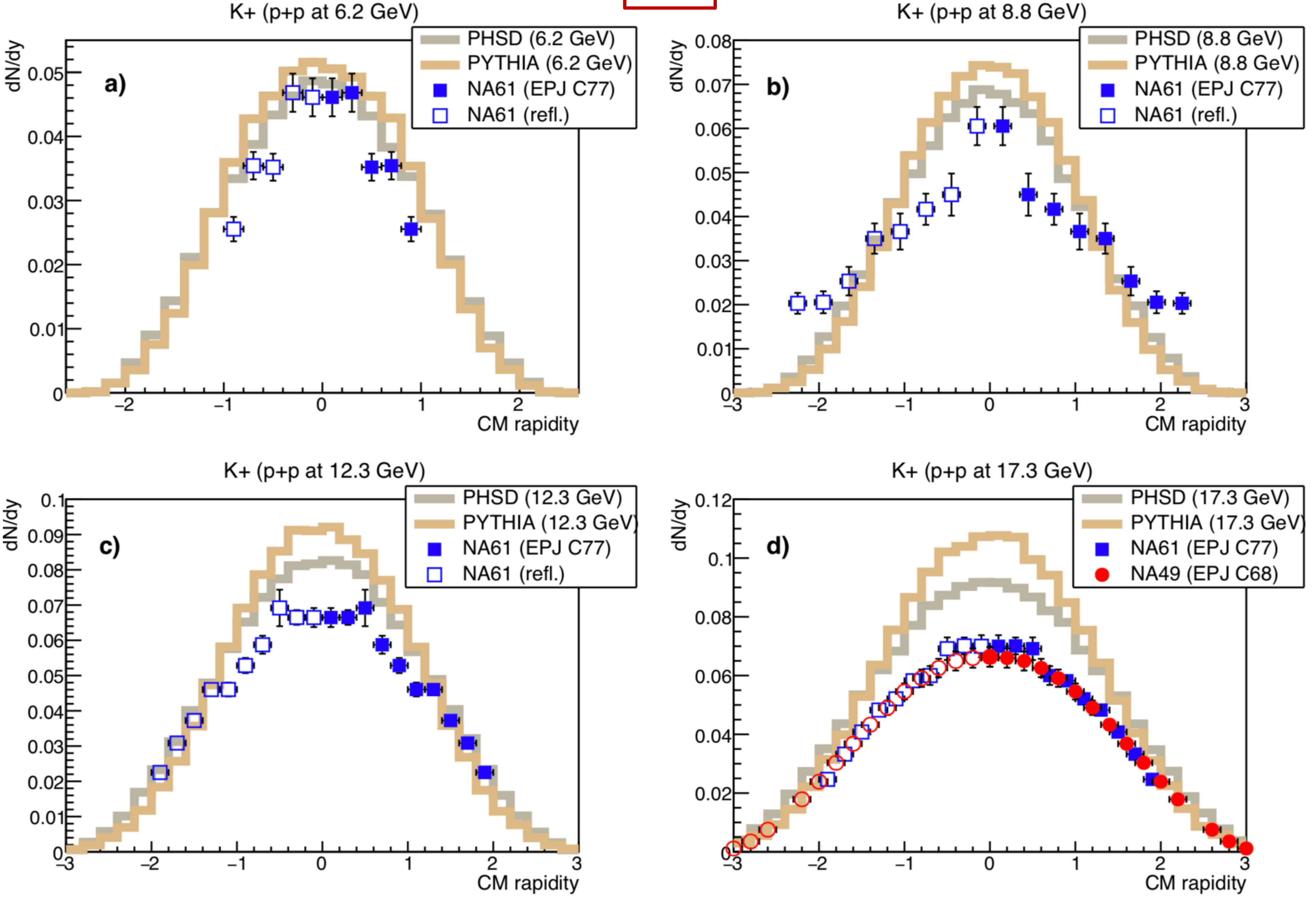
K+ (p+p at 6.2 GeV)
a)
PHSD (6.2 GeV)
PYTHIA (6.2 GeV)
NA61 (EPJ C77)
NA61 (refl.)
dN/dy
CM rapidity
K+ (p+p at 8.8 GeV)
b)
PHSD (8.8 GeV)
PYTHIA (8.8 GeV)
NA61 (EPJ C77)
NA61 (refl.)
dN/dy
CM rapidity
K+ (p+p at 12.3 GeV)
c)
PHSD (12.3 GeV)
PYTHIA (12.3 GeV)
NA61 (EPJ C77)
NA61 (refl.)
dN/dy
CM rapidity
K+ (p+p at 17.3 GeV)
d)
PHSD (17.3 GeV)
PYTHIA (17.3 GeV)
NA61 (EPJ C77)
NA49 (EPJ C68)
dN/dy
CM rapidity

p

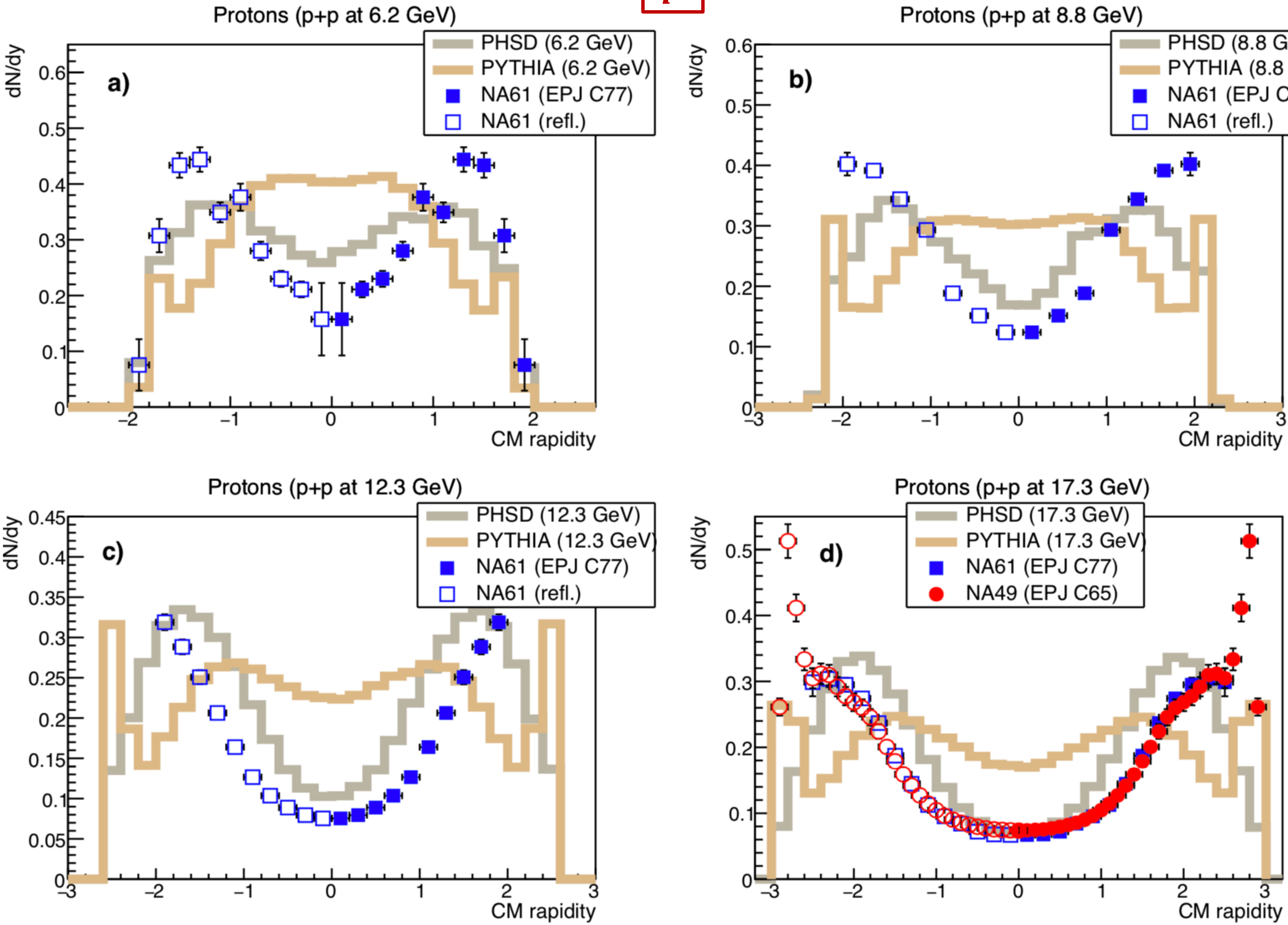
Protons (p+p at 6.2 GeV)
a)
PHSD (6.2 GeV)
PYTHIA (6.2 GeV)
NA61 (EPJ C77)
NA61 (refl.)
dN/dy
CM rapidity
Protons (p+p at 8.8 GeV)
b)
PHSD (8.8 GeV)
PYTHIA (8.8 GeV)
NA61 (EPJ C77)
NA61 (refl.)
dN/dy
CM rapidity
Protons (p+p at 12.3 GeV)
c)
PHSD (12.3 GeV)
PYTHIA (12.3 GeV)
NA61 (EPJ C77)
NA61 (refl.)
dN/dy
CM rapidity
Protons (p+p at 17.3 GeV)
d)
PHSD (17.3 GeV)
PYTHIA (17.3 GeV)
NA61 (EPJ C77)
NA49 (EPJ C65)
dN/dy
CM rapidity

Rapidity distributions

$\bar{p}$

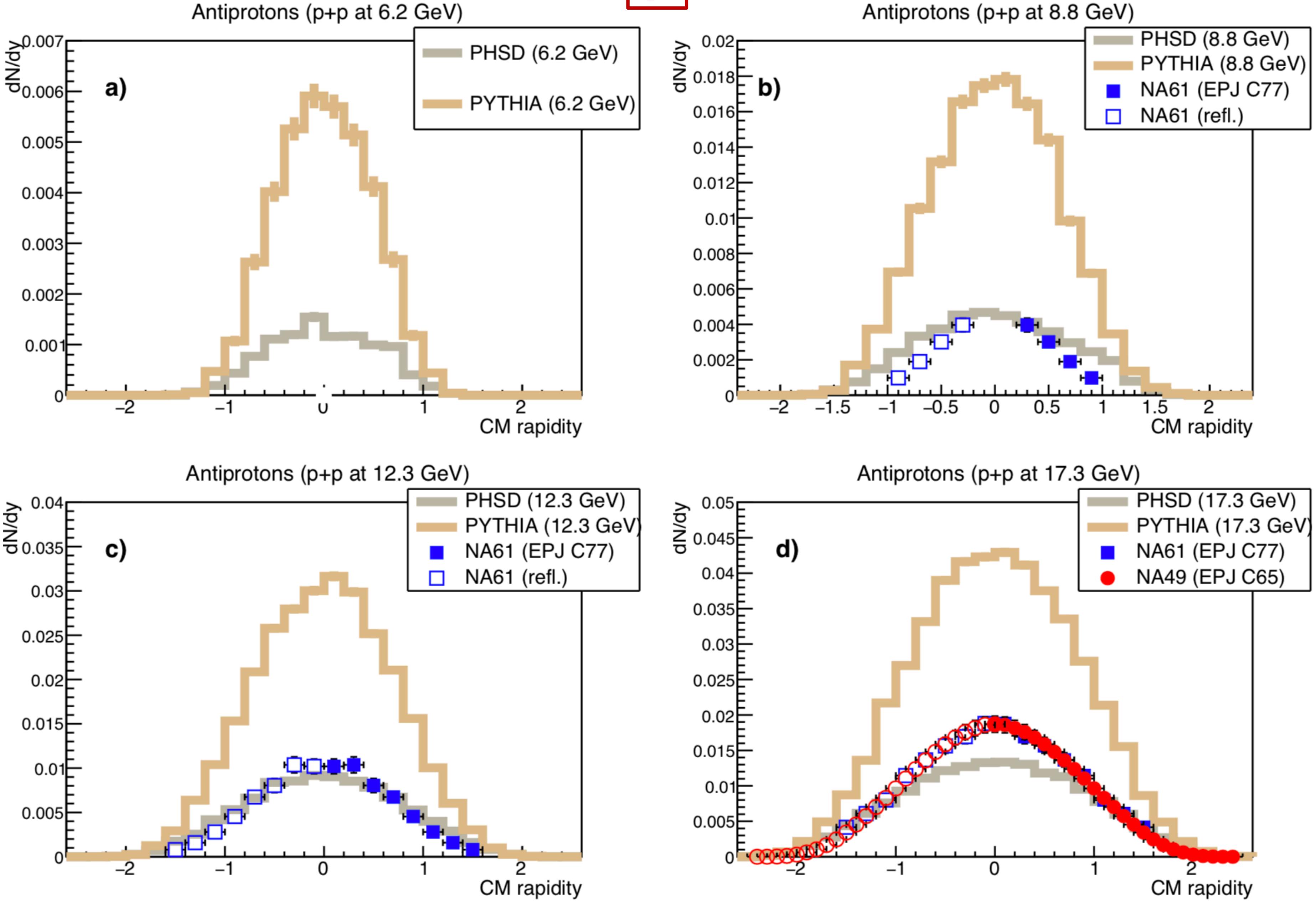

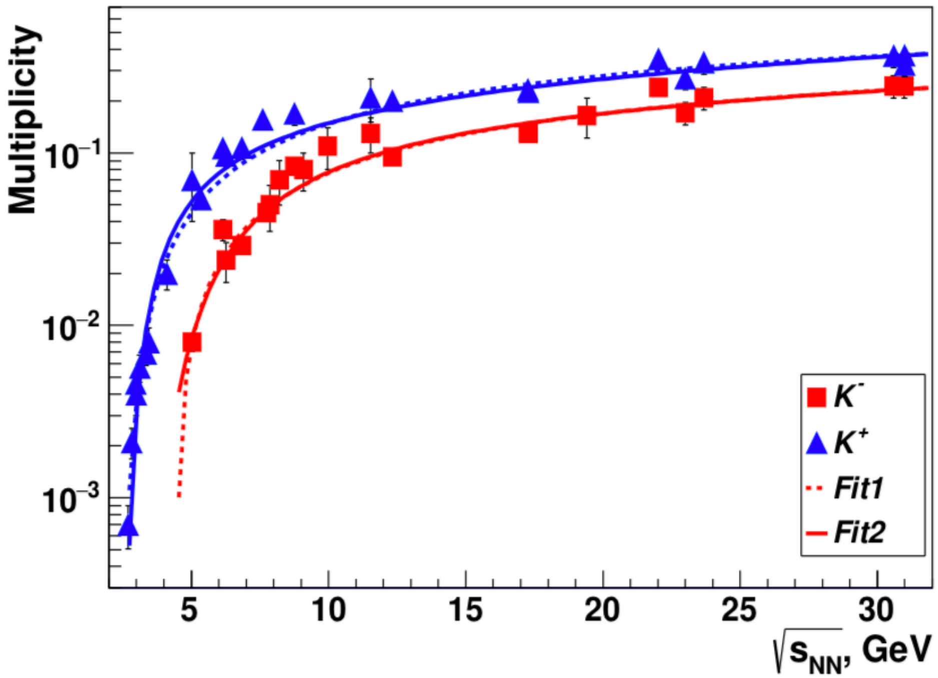

Strong dependence of $K^{\pm}$ production rates on $\sqrt{s}$ at low NICA energies

The relation between $K^{+}$and K^{-}along to the NICA energies is sensitive to strangeness production mechanisms. This is reflected in the K^{+}/K^{-}ratio depending on kinematic variables.

Both parameterizations describe the excitation function for kaons very good in the NICA energy range, but the overall trend is slightly better for the fit (2).

Two parametrizations are proposed to describe the excitation function of hadron production rates

$$\langle n_\pi \rangle = a + \frac{b}{\sqrt{s}} + c \ \ln s \quad (1)$$

← Based on a general analysis of hadron multiplicities including Redge trajectory with intercept one-half

$$\langle n \rangle = a(x-1)^b (x)^{-c} \quad (2)$$

← Based on the Lund String Model (LSM)

where $x = s/s_0$,
s: the square of the center-of-mass energy,
s_0: is the square of the production threshold.

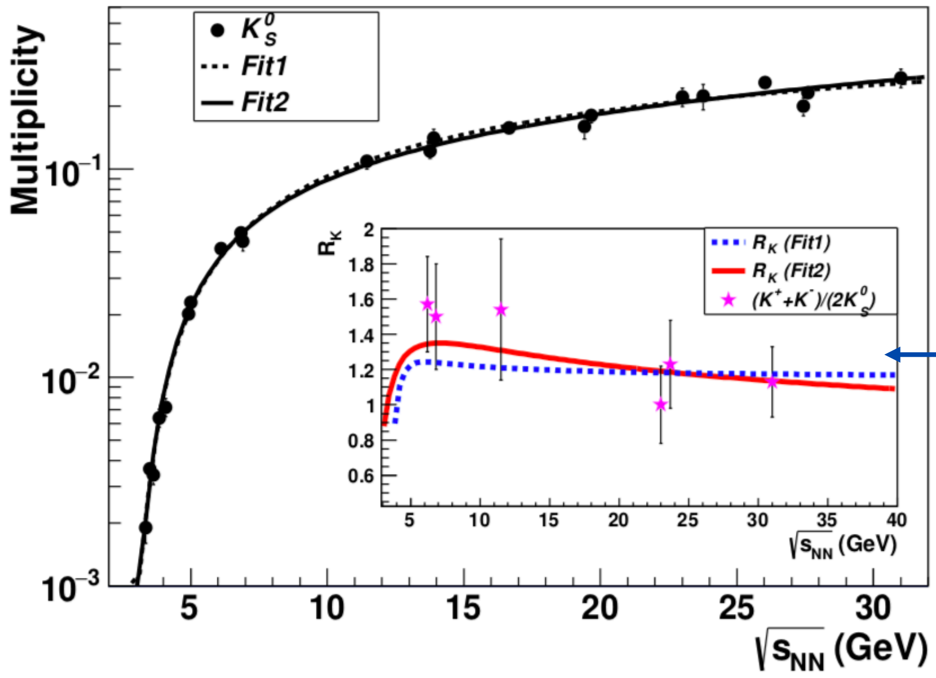

$$R_K = \frac{0.5(\langle n_{K^+}\rangle + \langle n_{K^-}\rangle)}{\langle n_{K^0_S}\rangle} \approx 1$$

Isospin invariance

R_K - energy dependence:

- Ratios of parameterized excitation function of kaon multiplicities according to the equation (1) and (2).

★ R_K calculated from experiments where K^+, K^-, K^0_S were measured at the same energy or at very closed energies

$R_K \to 1$ with the increasing $\sqrt{s}$ moving away from the isospin variance motivated kaon production ratio in the NICA energy range.

The trend of the experimental R_K is better described by the fit (2) based on the Lund String Model

No need for feed-down weak decay corrections in the case of kaons (contribution from Ω-hyperons is negligible at NICA energies)

Parameterizations of excitation functions of mean multiplicities

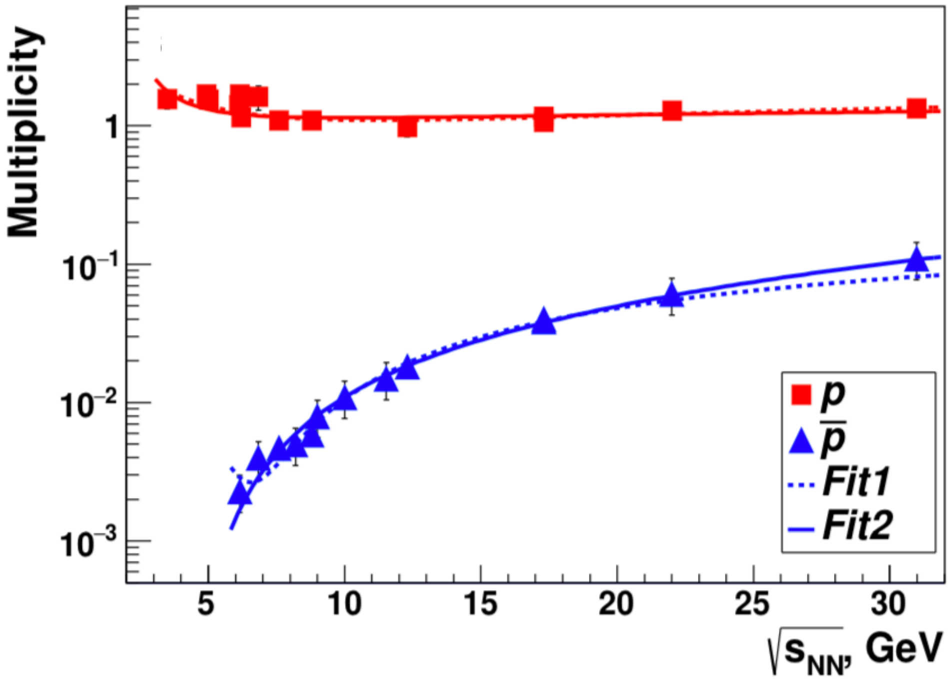

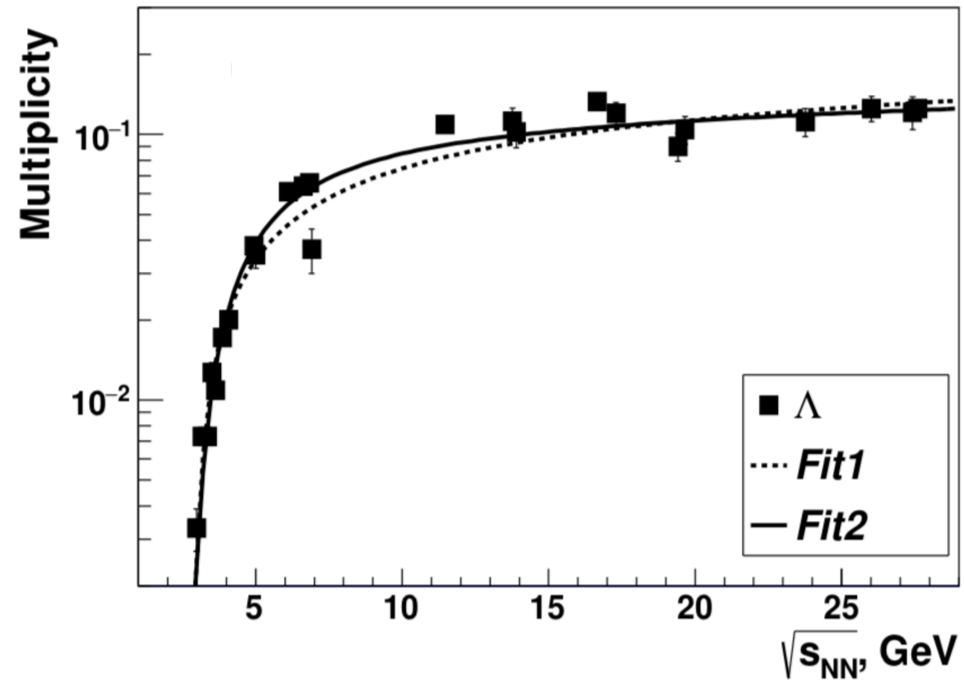

Poor amount of experimental data for mean multiplicity of $\boldsymbol{p}$ and $\overline{\boldsymbol{p}}$:

$\overline{\boldsymbol{p}}$: low production cross section
$\boldsymbol{p}$: Difficult to extrapolate rapidity distributions to the string fragmentation region (large rapidity)

Local minimum reached by $\boldsymbol{p}$ at ~10 GeV and then experiences a slow increase (increasing of the number of $B\bar{B}$ pairs)

Fast increase of $\overline{\boldsymbol{p}}$ at low energy

Fast increase of $\boldsymbol{\Lambda}$ yield close to the threshold and tends to the saturation at NICA energies (~10 GeV)

The data of $\overline{\boldsymbol{p}}$ and $\boldsymbol{\Lambda}$ are better described by the fit (2) based on the Lund String Model.

The data of **protons** are consistently described by both parameterizations (1) and (2).

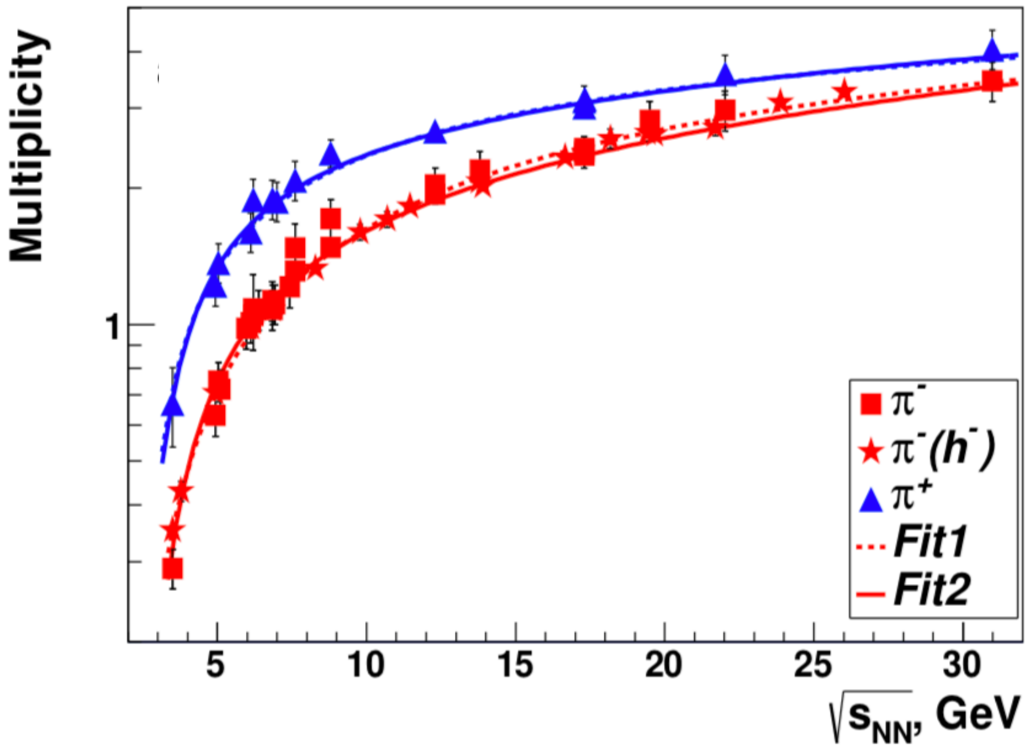

Pions represent the most abundant species!

The h^- method, to extract the $\langle \boldsymbol{n_{\pi^-}} \rangle$ from the negative charged hadrons, consists of subtracting $\langle n_{K^-} \rangle$ and $\langle n_{\bar{p}} \rangle$ at each $\sqrt{s}$ from the known (previously shown) energy dependences using the fit (2).

The data of $\boldsymbol{\pi}^+$ and $\boldsymbol{\pi}^-$ are consistently described by both parameterizations (1) and (2).

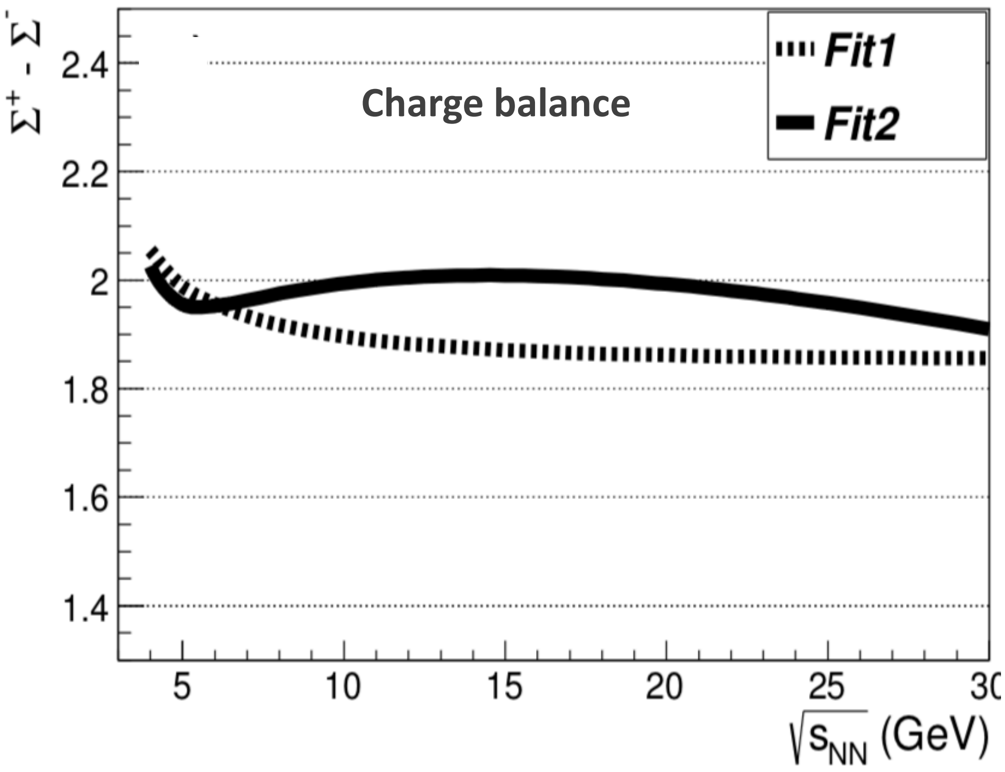

$$\Sigma^{+} - \Sigma^{-} \begin{cases} \Sigma^{+} = \langle n_{\pi^{+}} \rangle + \langle n_{K^{+}} \rangle + \langle n_{p} \rangle \\ \Sigma^{-} = \langle n_{\pi^{-}} \rangle + \langle n_{K^{-}} \rangle + \langle n_{\bar{p}} \rangle \end{cases}$$

Charge conservation in p + p reactions requires that $\Sigma^{+} - \Sigma^{-} = 2$

In this work the total charge balance is deviated from the nominal value (= 2) no more than 0.13 units. Thus, all the multiplicities computed from the parameterizations are in agreement with the charge conservation within 5.9% (Fit 1) and 1.5% (Fit 2).

Inclusive cross sections

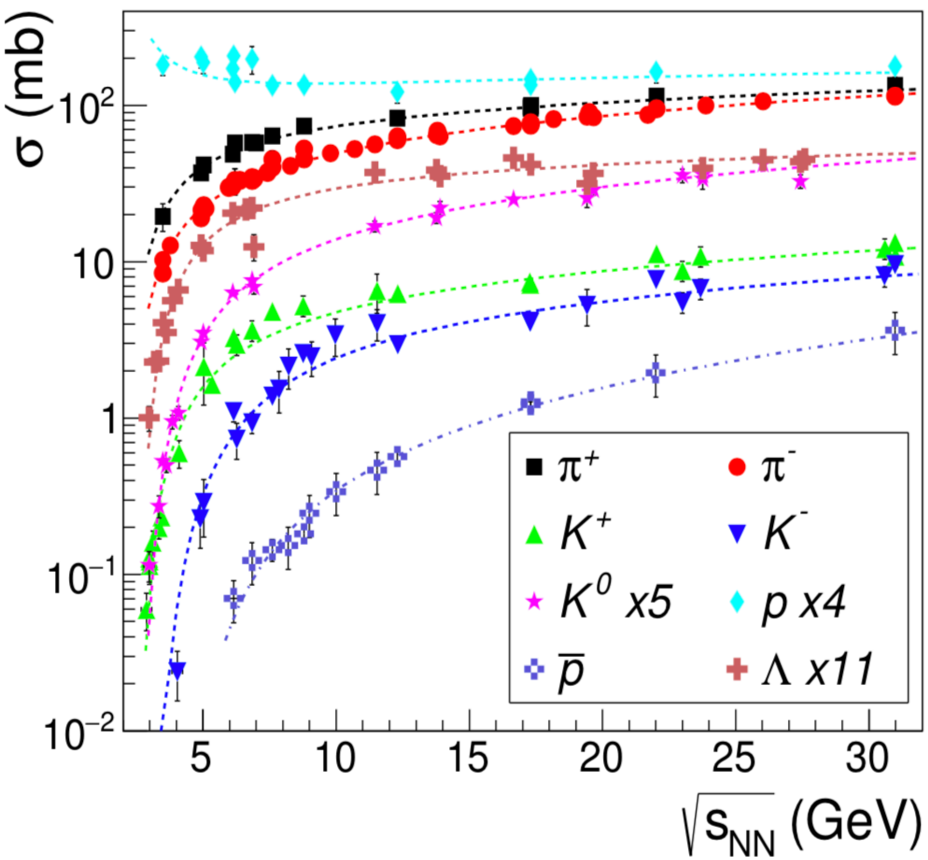

$\pi^{\pm}, K^{\pm}, K^0_s, \Lambda, p, \bar{p}$

$$\sigma = \langle n \rangle \sigma_{in}$$

$\langle n \rangle$: hadron multiplicity

σ_{in} : inelastic cross section

Based on the parametrization from: J. Phys. G 41 (2014) 019501

Fittings according the equation **(2)**:

$$\langle n \rangle = a(x-1)^b (x)^{-c}$$

Hadron	a	b	c	$s_0 (GeV^2)$	Chi2/NDF
π^-	18.79 ± 0.554	1.998 ± 0.089	$-.653 \pm 0.095$	4.64	0.5
π^+	43.046 ± 13.69	2.366 ± 1.386	2.168 ± 1.454	4.07	0.5
K^-	1.509 ± 0.363	5.138 ± 0.801	4.783 ± 0.853	8.2	2.0
K^+	2.176 ± 0.26	2.63 ± 0.155	2.285 ± 0.181	6.49	2.4
K^0_S	1.151 ± 0.087	3.697 ± 0.122	3.284 ± 0.139	6.49	1.9
p	19.49 ± 1.824	-8.717 ± 0.054	-8.823 ± 0.054	0	1.3
$\bar{p}$	0.122 ± 0.004	3.511 ± 0.291	2.69 ± 0.271	14.08	0.8
Λ	2.066 ± 0.161	2.625 ± 0.102	2.468 ± 0.121	6.49	4.1

Parameterizations of rapidity distributions

Rapidity distributions of π^-, K^-, π^+, K^+ scaled by the beam rapidity and normalized to the mean multiplicity $\langle n \rangle$.

Spectra of all energies together were fitted by single Gaussian functions: f(x) = p0 * exp (-(x - p1)*(x - p1) / 2. / p2 / p2)

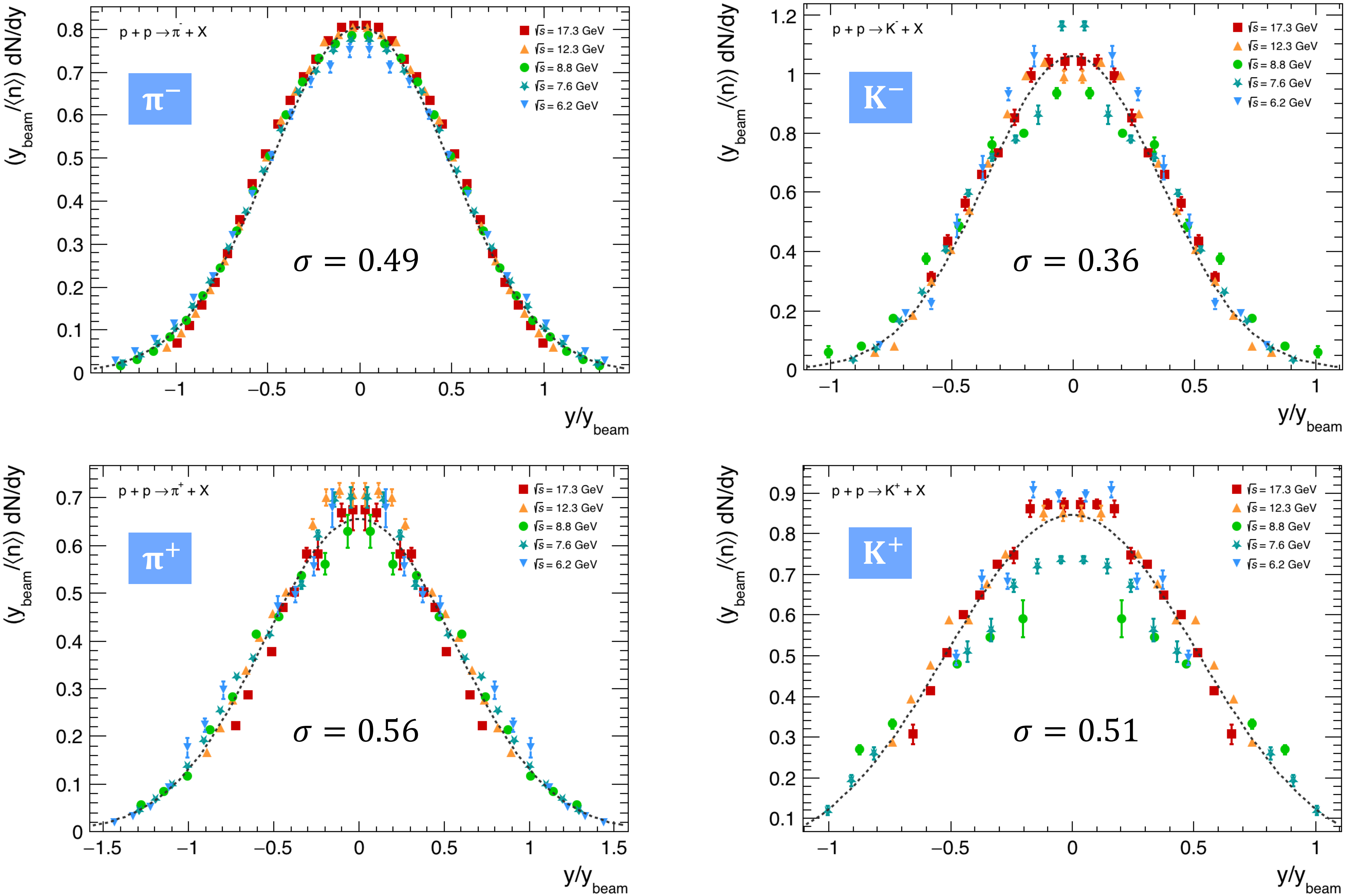

Parameterizations of rapidity distributions

Rapidity distributions of protons **scaled by the beam rapidity** and **normalized to the mean multiplicity $\langle n \rangle$**.

Spectra of all energies together were fitted by six order symmetric polynomial "pol6" (this is the simplest polynomial describing the data points).

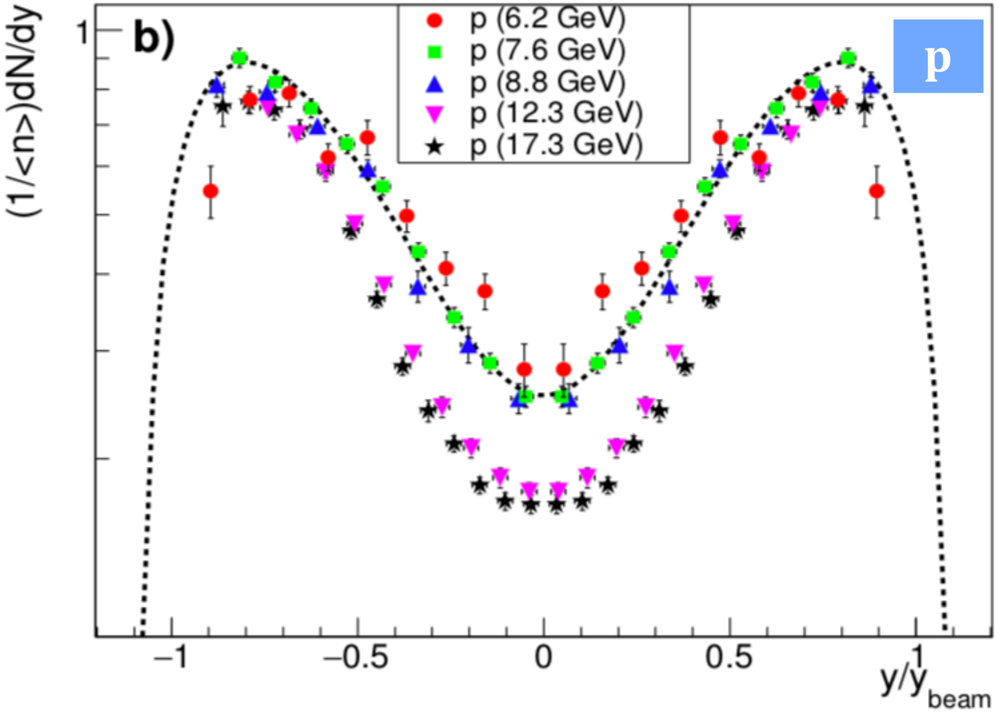

$$\frac{dN}{dy} \approx \underbrace{a(y/y_b)^6}_{} + \underbrace{b(y/y_b)^2 + c}_{}$$

a defines sharp fall-off of the rapidity spectra

b, ***c*** describe the behavior near mid-rapidity and normalization

The mid-rapidity dip is more pronounced as the energy increases, indicating an increasing of the momentum (rapidity) loss by the initial protons in the course of the reaction.

At lower energies the fragmentation peaks overlap in the rapidity space.

The gluon-gluon collisions are not relevant at these low (SPS) energies.

Effective temperature values of different hadrons as function of the normalized **rapidity ($y/y_{\mathbf{beam}}$)**, from Bose-Einstein distribution applied to the p_T distributions.

Measurements at all $\sqrt{s}$ = 6.2, 7.6, 12.3, 17.3 GeV were combined.

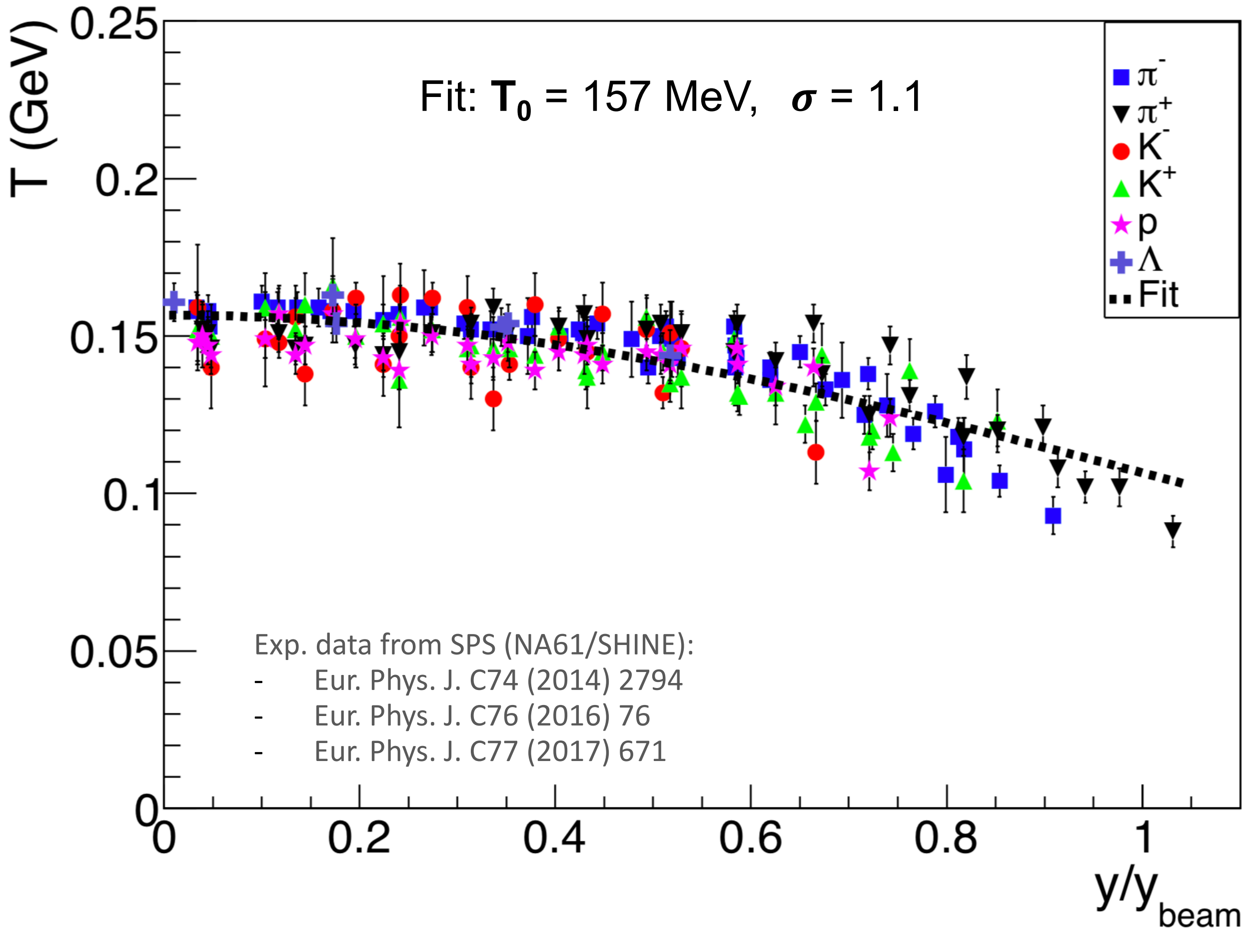

$\mathbf{T}$ $vs.$ $y/y_{\mathbf{beam}}$

- Gaussian shape at all energies and all hadrons ($\overline{p}$ not included)
- Little deviations between Gaussian shapes at $\sqrt{s} = 6 \div 17$ GeV

Deviation between Gaussians:

3%: amplitude (slope at mid-rapidity)
2%: standard deviation

- ✓ Experimental data on hadron yields from elementary inelastic collisions, i.e. p+p, have been compiled.

- ✓ A systematic study, based on this complete data set, is being performed in order to provide a complete evaluation of the energy dependence of the hadron production from p+p collisions at $4 < \sqrt{s} < 30$ GeV. New parameterizations for the excitation functions of mean multiplicities, rapidity spectra, and slope parameters of $\pi^{\pm}, K^{\pm}, K_S^0, \Lambda, p, \bar{p}$ are proposed.

- ✓ The analysis rely in the comparison with different model predictions.

- ✓ A new paper is under preparation.

A new review of excitation functions of hadron production in p+p collisions in the NICA energy range

V. Kolesnikov*, V. Kireyeu, V. Lenivenko, and K. Shtejer

Joint Institute for Nuclear Research, Dubna Russia

E. Bratkovskaya

GSI Helmholtzzentrum fur Schwerionenforschung GmbH, Planckstr. 1, 64291 Darmstadt, Germany and Institut fur Theoretische Physik, Johann Wolfgang Goethe-Universit, Max-von-Laue-Str. 1, 60438 Frankfurt am Main, Germany

Abstract

Data on hadron multiplicities from inelastic proton-proton interactions in the energy range of the NICA collider have been compiled. The compilation includes recent results from the NA61/SHINE and NA49 experiments at the SPS accelerator. New parameterizations for excitation functions of mean multiplicities $\langle\pi^{\pm}\rangle$, $\langle K^{\pm}\rangle$, $\langle K_S^0\rangle$, $\langle\Lambda\rangle$, $\langle p\rangle$, $\langle\bar{p}\rangle$ are obtained in the region of collision energies $3 < \sqrt{s_{NN}} < 30$ GeV. The energy dependence of the particle yields, as well as variation of rapidity and transverse momentum distributions are discussed. A correction method for the phase-space distributions of hadrons from microscopic models is suggested using an example of the PHQMD generator.

1 Introduction

The NICA accelerator complex is under construction at JINR (Dubna). It would offer a record luminosity (reaching 10^{27} cm^{-2}c^{-1}) for heavy-ion collisions in the energy range $4 < \sqrt{s_{NN}} < 11$ GeV [1]. Proton-proton collisions at NICA can be studied in the energy range from 4 to 25 GeV. The physics program of the MultiPurpose Detector (MPD) at the NICA collider is aimed at experimental exploration of a yet poorly known region of the QCD phase diagram of the highest net-baryon density with an emphasis on the nature of the transition from hadronic to quark-gluon degrees of freedom, modification of hadron properties in dense nuclear matter, and search for the signals about the critical end point [2]. However, the interpretation of experimental results from nucleus-nucleus interactions showing novel phenomena has to rely on comparison to the corresponding data from elementary collisions. For example, the excitation function of the strangeness-to-entropy ratio, which behaves differently in heavy-ion and p+p collisions, may serve as an important probe in the study of the deconfinement phase [3] or can be related to chiral symmetry restoration in the dense hadronic matter [4].

*Vadim.Kolesnikov@cern.ch

1

BACKUP

EPOS 1.99

Energy conserving quantum mechanical multiple scattering approach, based on **P**artons (partons ladders), **O**ff-shell remnants, and **S**plitting of parton ladders.

Unified formalism based on a combination of:

- Gribov – Regge theory
  - Focusses on the **soft** aspects of the particle collisions.
  - Describes multiple interactions using "Pomerons" representing an elementary interaction.
- Parton model
  - Introduces quarks and gluons giving a more precise description of interactions.
  - Uses QCD and QED descriptions to calculate cross sections of parton jets.
  - Parton production represented by Lund model strings.

Strengths:

- Consistent treatment of soft and hard scattering.
- Hard processes are introduced in a natural way without arbitrary assumptions (no artificial cuts)
- Energy conservation is considered in both, particle production and cross section calculation.
- Hydrodynamical evolution is done event by event.
- Treatment of participants and remnants ensures the energy conservation.

- **Data used to constrain parameters (~100) :**
  - string fragmentation : e+e- data,
  - hard Pomeron : DIS data,
  - soft Pomeron and vertices : pp,πp,Kp, pA cross sections
  - diffraction : pp low energy diffraction and multiplicity distributions
  - excitation functions : multiplicity in pp from SPS to LHC,
  - string ends and remnants : NA49 data
  - collective and screening effects : RHIC and LHC

EPOS designed to be used for particle physics experiment analysis (SPS, RHIC, LHC) for pp or Heavy Ion

Consistent treatment for all kind of systems: different contributions of particle production at different energies and rapidities (includes both: diffractive and inelastic scattering)!!!

Final state depends on the energy used for each event (multiplicity), not only on the energy available (collective hadronization when density of particles is high)

EPOS 1.99 can be used for minimum bias hadronic interaction generation from 100 GeV (lab) 1000 TeV (cms)

↓ $\sqrt{s} = 13.6$ GeV ↓ Air showers

- **One set of parameters for all energies and system**
  - not designed to be tuned by users

UrQMD 3.4

Ultra **R**elativistic **Q**uantum **M**olecular **D**ynamics

It is a non-equilibrium microscopic transport model for heavy ion collisions.

The underlying degrees of freedom are hadrons and strings

55 baryon and 32 meson species, ground state particles and all resonance with masses up to 2.25 GeV/c^2. Full particle-antiparticle, isospin and flavour SU(3) symetries are applied

Uses tables at low energies to properly describe data.

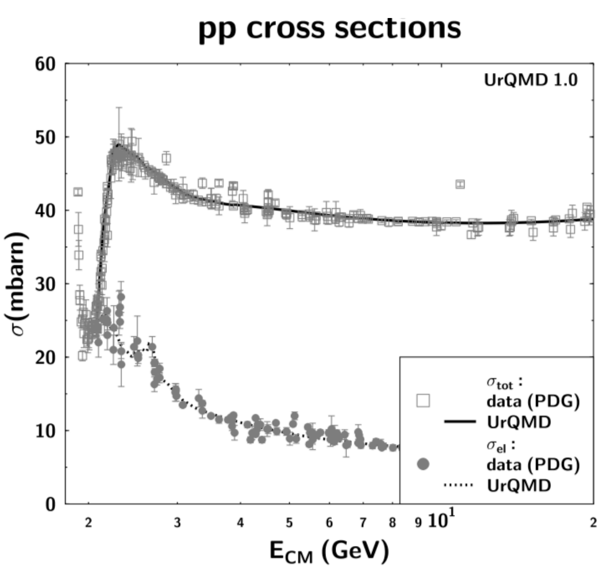

Time evolution in UrQMD

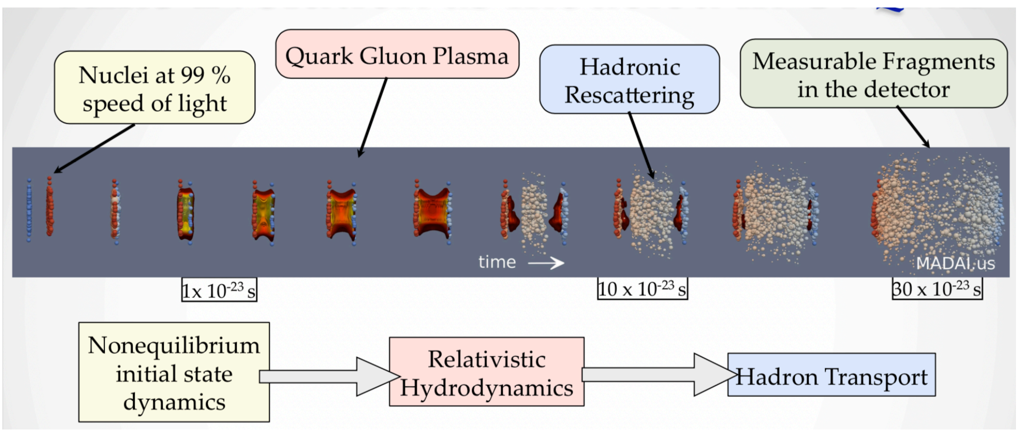

Hybrid approach is added for low energies and includes an ideal fluid-dynamic evolution for the hot and dense stage.

Time evolution of the distribution functions for particle species is described by a non-equilibrium approach based on an effective solution of the relativistic Boltzmann equation.

PHSD & UrQMD 3.4

PHSD, UrQMD } High energy inelastic hadron – hadron collisions are described by LUND string model via the FRITIOF routines } The two incoming hadrons emerge from the reaction as two excited color singlet states (strings)

LUND Model ⟹ It is a phenomenological model of hadronization, built upon a "string" analogy

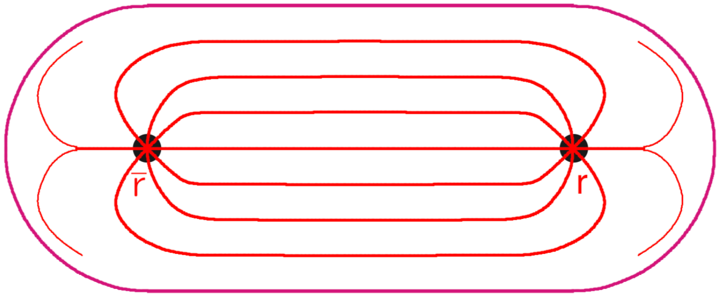

Partons are treated as field lines (except the highest-energy gluons) which are attracted to each other due to the gluon self interaction. These lines form a narrow tube (string) of strong color field.

The production probability *P* of massive $s\bar{s}$ pairs with respect to light flavor production ($u\bar{u}$, $d\bar{d}$) pairs follows the Schwinger formula.

$$\frac{P(s\bar{s})}{P(u\bar{u})} = \frac{P(s\bar{s})}{P(d\bar{d})} = \gamma_s = \exp\left(-\pi \frac{m_s^2 - m_q^2}{2k}\right)$$

$k \approx 1$ GeV/fm (string tension)

$m_{u,d,s}$: mass quarks

Default in FRITIOF routines: $\boldsymbol{\gamma_s \approx 0.3}$ ⟵ The suppression factor for strange quarks with regards to the light quarks

The strangeness production in p+p collisions at SPS energies is well reproduced in the LUND string model

PHSD & UrQMD 3.4

String fragmentation: the initial color connected parton pairs must break into smaller pieces, thus producing hadrons (when the stored potential energy is large enough)

Motion of quarks and antiquarks in a $q\bar{q}$ system

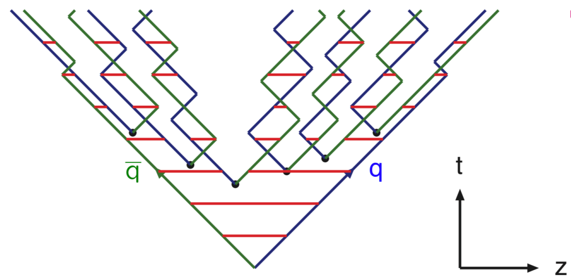

Fragmentation starts in the middle and spreads outwards

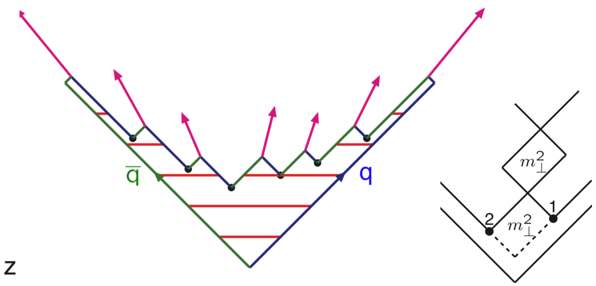

The produced hadron carries away some energy and momentum from the string according to the Lund symmetric fragmentation function:

$$f(z, m_T) \propto (1/z)(1-z)^a \exp(-b m_T^2 / z)$$

PHSD } Adopted the fragmentation function used in the LUND model, with: a = 0.23 and b = 0.34 GeV^{-2} for p+p and p+A collisions

UrQMD } Different fragmentation functions are used for leading nucleons and newly produced particles

$$f(z)_{nucl} = \exp\left(-\frac{(z-B)^2}{2A}\right)$$, for leading nucleons

$$f(z)_{prod} = (1-z)^2$$, for produced particles ⟵ Field-Feynman fragmentation function, with: A = 0.275 and B = 0.42